ventral prostate. *Toxicol Sci* 60: 132–143.
5. Couture L, Harris M, Birnbaum L (1990) Characterization of the peak period of sensitivity for the induction of hydronephrosis in C57BL/6N mice following exposure to 2,3,7,8-tetrachlorodibenzo-p-dioxin. *Fundam Appl Toxicol* 15: 142–150.
6. Schecter A, Olson J, Papke O (1996) Exposure of laboratory animals to polychlorinated dibenzodioxins and polychlorinated dibenzofurans from commercial rodent chow. *Chemosphere* 32: 501–508.
7. Guo Y, Hendrickx A, Overstreet J, Dieter J, Stewart D, Tarantal A, Laughlin L, Lasley B (1999) Endocrine biomarkers of early fetal loss in cynomolgus macaques (Macaca fascicularis) following exposure to dioxin. *Biol Reprod* 60: 707–713.
8. Ishimura R, Ohsako S, Miyabara Y, Sakaue M, Kawakami T, Aoki Y, Yonemoto J, Tohyama C (2002) Increased glycogen content and glucose transporter 3 mRNA level in the placenta of Holtzman rats after exposure to 2,3,7,8-tetrachlorodibenzo-p-dioxin. *Toxicol Appl Pharmacol* 178: 161–171.
9. Ishimura R, Ohsako S, Kawakami T, Sakaue M, Aoki Y, Tohyama C (2002) Altered protein profile and possible hypoxia in the placenta of 2,3,7,8-tetrachlorodibenzo-p-dioxin-exposed rats. *Toxicol Appl Pharmacol* 185: 197–206.
10. Pastorian K, Hawel L, Byus C (2000) Optimization of cDNA representational difference analysis for the identification of differentially expressed mRNAs. *Anal Biochem* 283: 89–98.
11. Mizutani T, Sonoda Y, Minegishi T, Wakabayashi K, Miyamoto K (1997) Cloning, characterization, and cellular distribution of rat scavenger receptor class B type I (SRBI) in the ovary. *Biochem Biophys Res Commun* 234: 499–505.
12. Sekiguchi T, Mizutani T, Yamada K, Yazawa T, Kawata H, Yoshino M, Kajitani T, Kameda T, Minegishi T, Miyamoto K (2002) Transcriptional regulation of the epiregulin gene in the rat ovary. *Endocrinology* 143: 4718–4729.
13. Mizutani T, Yamada K, Yazawa T, Okada T, Minegishi T, Miyamoto K (2001) Cloning and characterization of gonadotropin-inducible ovarian transcription factors (GIOT1 and -2) that are novel members of the (Cys)(2)-(His)(2)-type zinc finger protein family. *Mol Endocrinol* 15: 1693–1705.
14. Lancaster J, Dressman H, Whitaker R, Havrilesky L, Gray J, Marks J, Nevins J, Berchuck A (2004) Gene expression patterns that characterize advanced stage serous ovarian cancers. *J Soc Gynecol Investig* 11: 51–59.
15. Whitlock JJ (1999) Induction of cytochrome P4501A1. *Annu Rev Pharmacol Toxicol* 39: 103–125.
16. Whitlock JJ, Chichester C, Bedgood R, Okino S, Ko H, Ma Q, Dong L, Li H, Clarke-Katzenberg R (1997) Induction of drug-metabolizing enzymes by dioxin. *Drug Metab Rev* 29: 1107–1127.
17. Angiolillo A, Sgadari C, Taub D, Liao F, Farber J, Maheshwari S, Kleinman H, Reaman G, Tosato G (1995) Human interferon-inducible protein 10 is a potent inhibitor of angiogenesis *in vivo*. *J Exp Med* 182: 155–162.
18. Strieter R, Kunkel S, Arenberg D, Burdick M, Polverini P (1995) Interferon gamma-inducible protein 10 (IP-10), a member of the C-X-C chemokine family, is an inhibitor of angiogenesis. *Biochem Biophys Res Commun* 210: 51–57.
19. Singh U, Singh S, Iqbal N, Weaver C, McGhee J, Lillard JJ (2003) IFN-gamma-inducible chemokines enhance adaptive immunity and colitis. *J Interferon Cytokine Res* 23: 591–600.
20. Neumann B, Emmanuilidis K, Stadler M, Holzmann B (1998) Distinct functions of interferon-gamma for chemokine expression in models of acute lung inflammation. *Immunology* 95: 512–521.
21. Semenza G (1999) Regulation of mammalian O2 homeostasis by hypoxia-inducible factor 1. *Annu Rev Cell Dev Biol* 15: 551–578.
22. Leonard W (2001) Role of Jak kinases and STATs in cytokine signal transduction. *Int J Hematol* 73: 271–277.
23. Yu-Lee L (2002) Prolactin modulation of immune and inflammatory responses. *Recent Prog Horm Res* 57: 435–455.
24. Southard J, Talamantes F (1991) Placental prolactin-like proteins in rodents: variations on a structural theme. *Mol Cell Endocrinol* 79: 133–140.
25. Friesel R, Komoriya A, Maciag T (1987) Inhibition of endothelial cell proliferation by gamma-interferon. *J Cell Biol* 104: 689–696.
26. Good D, Polverini P, Rastinejad F, Le Beau M, Lemons R, Frazier W, Bouck N (1990) A tumor suppressor-dependent inhibitor of angiogenesis is immunologically and functionally indistinguishable from a fragment of thrombospondin. *Proc Natl Acad Sci USA* 87: 6624–6628.
27. Takigawa M, Nishida Y, Suzuki F, Kishi J, Yamashita K, Hayakawa T (1990) Induction of angiogenesis in chick yolk-sac membrane by polyamines and its inhibition by tissue inhibitors of metalloproteinases (TIMP and TIMP-2). *Biochem Biophys Res Commun* 171: 1264–1271.

Molecular and Cellular Biology, Jan. 2005, p. 136–146 Vol. 25, No. 1
0270-7306/05/$08.00+0 doi:10.1128/MCB.25.1.136–146.2005
Copyright © 2005, American Society for Microbiology. All Rights Reserved.

Cyclic AMP Potentiates Vascular Endothelial Cadherin-Mediated Cell-Cell Contact To Enhance Endothelial Barrier Function through an Epac-Rap1 Signaling Pathway

Shigetomo Fukuhara,[1] Atsuko Sakurai,[1] Hideto Sano,[2] Akiko Yamagishi,[1] Satoshi Somekawa,[1,3] Nobuyuki Takakura,[2] Yoshihiko Saito,[3] Kenji Kangawa,[4] and Naoki Mochizuki[1]*

Department of Structural Analysis[1] and Department of Biochemistry,[4] National Cardiovascular Center Research Institute, Osaka, Department of Stem Cell Biology, Cancer Research Institute, Kanazawa University, Kanazawa,[2] and First Department of Internal Medicine, Nara Medical University, Nara,[3] Japan

Received 2 August 2004/Returned for modification 2 September 2004/Accepted 28 September 2004

Cyclic AMP (cAMP) is a well-known intracellular signaling molecule improving barrier function in vascular endothelial cells. Here, we delineate a novel cAMP-triggered signal that regulates the barrier function. We found that cAMP-elevating reagents, prostacyclin and forskolin, decreased cell permeability and enhanced vascular endothelial (VE) cadherin-dependent cell adhesion. Although the decreased permeability and the increased VE-cadherin-mediated adhesion by prostacyclin and forskolin were insensitive to a specific inhibitor for cAMP-dependent protein kinase, these effects were mimicked by 8-(4-chlorophenylthio)-2′-*O*-methyladenosine-3′, 5′-cyclic monophosphate, a specific activator for Epac, which is a novel cAMP-dependent guanine nucleotide exchange factor for Rap1. Thus, we investigated the effect of Rap1 on permeability and the VE-cadherin-mediated cell adhesion by expressing either constitutive active Rap1 or Rap1GAPII. Activation of Rap1 resulted in a decrease in permeability and enhancement of VE-cadherin-dependent cell adhesion, whereas inactivation of Rap1 had the counter effect. Furthermore, prostacyclin and forskolin induced cortical actin rearrangement in a Rap1-dependent manner. In conclusion, cAMP-Epac-Rap1 signaling promotes decreased cell permeability by enhancing VE-cadherin-mediated adhesion lined by the rearranged cortical actin.

Endothelial cells lining blood vessels regulate endothelial barrier function, which restricts the passage of plasma proteins and circulating cells across the endothelial cells. Endothelial barrier dysfunction results in an increase in vascular permeability, thereby causing edema or inflammatory or metastatic cell infiltration. Inflammatory mediators such as thrombin and histamine induce intercellular gap formation, leading to an increase in endothelial permeability (1, 4). In contrast, angiopoietin 1 and sphingosine-1-phosphate (S1P) stabilize endothelial barrier integrity (17, 18). In addition, cyclic AMP (cAMP), a second messenger downstream of Gs-coupled receptor, improves endothelial cell barrier function (32, 39, 43). Consistently, cAMP-elevating G protein-coupled receptor (GPCR) agonists, adrenomedullin (AM), prostacyclin (PGI2), prostaglandin E2 (PGE2), and β-adrenergic agonists reduce endothelial hyperpermeability induced by inflammatory stimuli (15, 19, 25).

The endothelial cell barrier is structurally organized by adherens junctions (AJ) and tight junctions. Vascular endothelial (VE) cells express both VE-cadherin (also known as cadherin-5 and CD144) and neural (N)-cadherin (9, 33). VE-cadherin constitutes AJ, whereas N-cadherin formed the cell-cell contacts between endothelial cells and endothelial cell-supporting pericytes. VE-cadherin mediates calcium-dependent, homophilic intercellular adhesion. Its short cytoplasmic tail binds to three armadillo family proteins, β-, γ-, and p120-catenins. β- and γ-catenins associated with α-catenin link the VE-cadherin complex to the actin cytoskeleton and, therefore, strengthen the AJ adhesiveness (9).

Endothelial AJ are dynamic structures, and their adhesive property is finely regulated by several different mechanisms. Tyrosine phosphorylation of VE-cadherin, β-catenin, and p120-catenin correlates with weakened endothelial cell-cell adhesion. VE growth factors and inflammatory mediators such as histamine and thrombin induce tyrosine phosphorylation of AJ components, resulting in the weakened cell-cell contacts and increased endothelial cell permeability (1, 14, 40). In clear contrast, angiopoietin 1, which stabilizes cell-cell contacts, induces dephosphorylation of endothelial cell adhesion molecules, VE-cadherin, and platelet endothelial cell adhesion molecule 1 (17). It has been also reported that S1P induces AJ formation and enhances barrier function through a Rac-dependent cortical actin rearrangement (18). cAMP-dependent protein kinase A (PKA) is suggested to be crucial for cAMP-triggered stabilization of cell-cell contacts and for barrier integrity of endothelial cells (43). However, it has not been clear whether PKA-independent signaling is involved in the regulation of endothelial barrier function.

Rap1, belonging to Ras family GTPase, is involved in the formation and stabilization of AJ in *Drosophila melanogaster* (23). Rap1 becomes the GTP-bound active form by guanine

* Corresponding author. Mailing address: Department of Structural Analysis, National Cardiovascular Center Research Institute, 5-7-1 Fujishirodai, Suita, Osaka 565-8565, Japan. Phone: 81-6-6833-5012, ext. 2508. Fax: 81-6-6835-5461. E-mail: nmochizu@ri.ncvc.go.jp.

nucleotide exchange factor (GEF) and the GDP-bound inactive form by GTPase-activating proteins (GAP), respectively. GEFs for Rap1 include C3G, CalDAG-GEFs, Epacs, and DOCK4 (reviewed in reference 6). DOCK4, which is disrupted in various types of human cancers, regulates the formation of AJ (41). Very recent reports also revealed that Rap1 activity is required for the formation of E-cadherin-based cell-cell contacts (20, 36). These findings prompted us to investigate how Rap1 is activated to stabilize cell-cell contacts and to examine the physiological consequence of stabilized cell-cell contacts by Rap1.

In the present study, we investigated the mechanism by which cAMP-elevating GPCR agonists potentiate endothelial barrier function and restrict cell permeability. We found that increased cAMP triggers Epac-Rap1 signaling to reduce permeability independently of PKA by augmentation of VE-cadherin-mediated cell-cell adhesion.

MATERIALS AND METHODS

Reagents and antibodies. Human recombinant AM was kindly provided by Shionogi & Co. Ltd (31). Materials were purchased as follows: isoproterenol (Iso), PGE2, PGI2, thrombin, forskolin (FSK), and 3-isobutyl-1-methylxanthine (IBMX) from Wako Pure Chemical Industries; dibutyryl-cAMP (dbcAMP) from Sigma-Aldrich; H89 from Seikagaku Corporation; 8-(4-chlorophenylthio)-2′-*O*-methyladenosine-3′,5′-cyclic monophosphate (8-CPT-2′-O-Me-cAMP) from Tocris; fluorescein isothiocyanate (FITC)-labeled dextran (molecular weight, 42,000) and purified human immunoglobulin G (IgG) Fc protein from ICN Biologicals; vascular endothelial growth factor (VEGF) from R & D Systems. Anti-Rap1GAPII antibody was developed by immunization of glutathione *S*-transferase (GST)-tagged Rap1GAPII (amino acids 411 to 694 of Rap1GAPII). Other antibodies used here were purchased as follows: anti-VE-cadherin from Chemicon International and Transduction Laboratories; anti-β-catenin from Transduction Laboratories; anti-CREB and anti-phospho-CREB (Ser133) from Cell Signaling Technology; anti-Rap1 from Santa Cruz Biotechnology; anti-cortactin from Upstate Biotechnology, Inc.; rhodamine-phalloidin and Alexa 488-labeled goat anti-mouse IgG from Molecular Probes; horseradish peroxidase-coupled goat anti-mouse and goat anti-rabbit IgG from Amersham Biosciences.

Cell culture and transfection. Human umbilical vein endothelial cells (HUVECs) and human arterial endothelial cells (HAECs) were purchased from Kurabo (Kurashiki, Japan). The cells were maintained in HuMedia-EG2 with a growth additive set as described previously (12) and used for experiments before passages 7 and 10, respectively. HEK293, 293T, and HeLa cells were maintained in Dulbecco's modified Eagle's medium (DMEM; Nissui, Tokyo, Japan) supplemented with 10% fetal bovine serum and antibiotics (100 μg of streptomycin/ml and 100 U of penicillin/ml). HUVECs and 293T cells were transfected by using Lipofectamine Plus reagent (Invitrogen) and by the calcium-phosphate precipitation technique, respectively.

Plasmids and adenovirus. pcDNA-VE-cad-Ect-Fc-His is a modified vector of pcDNA3.1-Fc-PECAM-1 (a kind gift from W. A. Muller, Cornell University) for producing the secreted form of the extracellular domain of VE-cadherin fused with Fc followed by a six-His tag. A DNA fragment encoding human Epac lacking the cAMP binding domain (amino acids 324 to 881) was amplified by PCR with pMT2SM-HA-Epac (a kind gift from J. L. Bos, Utrecht University, Utrecht, The Netherlands) as a template and ligated into the pCXN2 vector (12). pCXN2-FLAG-Rap1V12-IRES-EGFP expressed both FLAG-tagged Rap1V12 and internal ribosomal entry site (IRES)-driven enhanced green fluorescent protein (EGFP), and pCXN2-Rap1GAPII-IRES-EGFP expressed both FLAG-tagged Rap1GAPII and IRES-driven EGFP. pGL3 control vector was purchased from Promega Corp. Recombinant adenoviruses encoding Rap1GAPII (Ad-RapGAP) and LacZ (Ad-LacZ) were obtained from S. Hattori (The Institute of Medical Science, University of Tokyo) and M. Matsuda (Research Institute for Microbial Disease, Osaka University, Osaka, Japan), respectively. Adenoviruses expressing FLAG-tagged Rap1V12 and IRES-driven EGFP (Ad-Flag-Rap1V12-IRES-EGFP) were produced by using the Adeno-X system according to the manufacturer's protocol (Clontech). Endothelial cells were infected with adenoviruses at the appropriate multiplicities of infection (MOI) as described in the figure legends.

Permeability assay. Permeability across the endothelial cell monolayer was measured by using type I collagen-coated transwell units (6.5-mm diameter, 3.0-μm-pore-size polycarbonate filter; Corning Costar Corporation). HUVECs plated at 10^5 cells in each well were cultured for 3 to 4 days before experiments. After serum starvation in medium 199 containing 1% bovine serum albumin (BSA) for 1 h, the cells were treated with the agonists or drugs, as indicated in the figure legends, for 30 min. Permeability was measured by adding 1 mg of FITC-labeled dextran (molecular weight, 42,000)/ml together with or without 2 U of thrombin/ml to the upper chamber. After incubation for 30 min, 50 μl of sample from the lower compartment was diluted with 300 μl of phosphate-buffered saline (PBS) and measured for fluorescence at 520 nm when excited at 492 nm with a spectrophotometer F-4500 (Hitachi). HUVECs infected with adenovirus for 24 h after becoming confluent and kept for another 24 h in replaced medium were subjected to a cell permeability assay.

Immunocytochemistry. Monolayer-cultured HUVECs grown on a 35-mm-diameter glass base dish (Asahi Techno Glass) were starved in medium 199 containing 0.5% BSA for 3 h and subsequently incubated with the stimulants indicated in the figure legends for 30 min. After stimulation, the cells were fixed in PBS containing 2% formaldehyde for 30 min at 4°C, washed with PBS, and permeabilized with 0.05% Triton X-100 for 30 min at 4°C. Cells were blocked with PBS containing 4% BSA for 1 h at room temperature (RT) and stained with rhodamine-phalloidin for 20 min, anti-VE-cadherin for 60 min, and anticortactin for 60 min at RT. Protein reacting with antibody was visualized with Alexa 488-labeled goat anti-mouse IgG. Images were recorded with a confocal microscope (BX50WI, Fluoview; Olympus) with a water immersion objective lens (LUMPlanFl 100X1.00W).

VE-cadherin translocation assay and Western blot analysis. HUVECs plated in six-well plates were serum starved in medium 199 containing 1% BSA overnight. The cells were stimulated with PGI2 and FSK for the indicated time and fractionated with cytoskeleton-stabilizing buffer (10 mM HEPES [pH 7.4], 250 mM sucrose, 150 mM KCl, 1 mM EGTA, 3 mM $MgCl_2$, 1× protease inhibitor cocktail [Roche Diagnostics], 1 mM Na_3VO_4, 0.5% Triton X-100) by centrifugation at 15,000 × *g* for 15 min. The Triton X-100-insoluble fraction was subjected to sodium dodecyl sulfate-polyacrylamide gel electrophoresis (SDS-PAGE) followed by transfer to Immobilon-P (Amersham Biosciences) and immunoblotting with the indicated antibodies. Immunocomplexes were visualized by enhanced chemiluminescence detection (Amersham Biosciences) with species-matched peroxidase-conjugated secondary antibodies.

Purification of recombinant VE-cadherin ectodomain-Fc chimeric protein. 293T cells transfected with pcDNA-VE-cad-Ect-Fc-His were cultured in DMEM supplemented with 10% fetal calf serum for 24 h and subsequently kept in replaced medium (DMEM-F21 containing 1% fetal calf serum) for 7 days. VE-cadherin-Fc (VEC-Fc) protein secreted into the medium was collected every 2 days and centrifuged to remove floating cells and debris. VEC-Fc was collected on ProBond resin (Invitrogen) by gentle agitation overnight at 4°C. VEC-Fc protein bound to the beads was eluted with 500 mM imidazole, concentrated with Amicon Centriplus 30 (Millipore), and buffer exchanged into PBS containing 2 mM $CaCl_2$ and 2 mM $MgCl_2$ (PBS-Ca/Mg) by dialysis.

Cell adhesion assay. Twenty-four-well tissue culture plates were coated with 10 μg of VEC-Fc or Fc protein/ml in PBS-Ca/Mg at 4°C overnight. After washing with PBS-Ca/Mg, the plates were blocked with 1% heat-inactivated BSA in PBS (heat inactivated at 85°C for 12 min) for 1 h at RT. To examine cell adhesion to the VEC-Fc- or Fc-coated dish, cells were suspended in 0.5% BSA-containing medium 199 and incubated for 30 min at 37°C. Cells (1.5×10^5) were plated on each VEC-Fc- or Fc-coated well in the presence or absence of agonists, drugs, and 5 mM EGTA and adhered to the dish at 37°C for the indicated time. To analyze cell adhesion to a collagen-covered surface, cells were plated onto a collagen-coated six-well plate (Iwaki) and adhered to the dish in the presence or absence of 5 mM EGTA. After washing with PBS-Ca/Mg four times to remove nonadherent cells, adherent cells and input cells were quantified by measuring endogenous alkaline phosphatase activity as described elsewhere (35). Briefly, the cells were lysed in a buffer containing 100 mM Tris-citrate (pH 6.5) and 0.25% Triton X-100, and alkaline phosphate activity in the lysate was measured by using the AttoPhos AP fluorescent substrate system (Promega Corp.). To examine the effects of Rap1V12, EpacΔcAMP, and Rap1GAPII, HUVECs were transfected with plasmids encoding either Rap1V12, EpacΔcAMP, or Rap1GAPII together with the luciferase reporter construct (pGL3 control vector). The adhesion of cells expressing Rap1V12, EpacΔcAMP, or Rap1GAPII to the VEC-Fc-coated dish was normalized by measuring the luciferase activity of the cells and input cells (16).

Detection of GTP-bound form of Rap1. Rap1 activity was assessed by a modified Bos's method as described previously (34). Briefly, HUVECs starved in medium 199 containing 1% BSA overnight were stimulated with the indicated

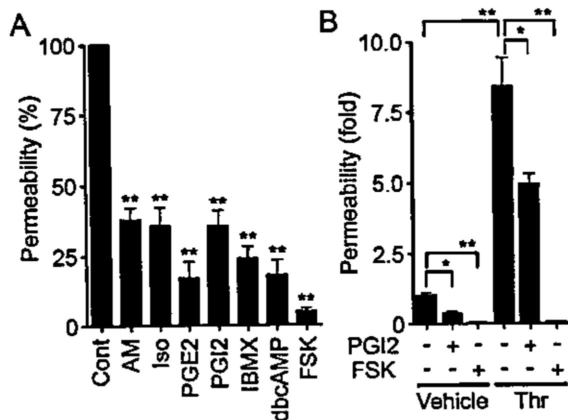

FIG. 1. cAMP enhances barrier function of monolayer VE cells. (A) Vascular permeability, reflecting barrier function, was analyzed by measuring the fluorescence of FITC-labeled dextran across the monolayer-cultured HUVECs as described in Materials and Methods. HUVECs grown on transwell filters were incubated with control (Cont), 0.1 μM AM, 200 μM Iso, 200-ng/ml PGE2, 10-μg/ml PGI2, 1 mM IBMX, 1 mM dbcAMP, and 10 μM FSK for 30 min. Average permeability ± standard deviation is expressed as a percentage compared to the control. (B) The effects of PGI2 and FSK on vascular permeability were quantified in the presence (+) or absence (−) (Vehicle) of 2 U of thrombin (Thr)/ml. Average permeability ± standard deviation is expressed as the increase relative to that observed in unstimulated HUVECs in the vehicle. Data shown are the results from at least three independent experiments. Significant differences from the control (A) or between two groups (B) determined by Student's t test are indicated by a single asterisk ($P < 0.05$) or double asterisks ($P < 0.01$).

agonists and drugs and lysed at 4°C in a pull-down lysis buffer (20 mM Tris-HCl [pH 7.5], 100 mM NaCl, 10 mM $MgCl_2$, 1% Triton X-100, 1 mM EGTA, 1 mM dithiothreitol, 1 mM Na_3VO_4, 1× protease inhibitor cocktail). GTP-bound Rap1 was collected on the GST-Rap1 binding domain of RalGDS precoupled to glutathione-Sepharose beads and subjected to SDS-PAGE followed by immunoblotting with anti-Rap1.

In vivo permeability assay. In vivo permeability was quantified by a modified Miles assay as described previously (29). In brief, ICR mice (Japan SLC, Inc.) shaved 3 days before experiments were lightly anesthetized and intravenously injected with 150 μl of 1% Evans blue dye solution (in saline) passed through a 0.22-μm-pore-size filter. Fifteen minutes later, 20 μl of PBS, VEGF (50 μg/ml), and/or 8-CPT-2′-O-Me-cAMP (1 mM) were applied by intradermal injections with a 30-gauge needle. The sites of intradermal injection were photographed 60 min after the injection, carefully dissected, and weighed. To quantify the vascular permeability, extravasated blue dye was eluted from the dissected skin with formamide at 56°C, and optical density was measured by spectrophotometry at 620 nm.

RESULTS

cAMP enhances the barrier property of monolayer-cultured endothelial cell. To evaluate the barrier function, we examined the permeability of FITC-labeled dextran across monolayer HUVECs. Expectedly, AM, Iso, PGE2, and PGI2 reduced basal endothelial permeability in HUVECs (Fig. 1A). PGI2 also reduced thrombin-induced vascular permeability (Fig. 1B). Other cAMP-elevating bio-ligands similarly reduced thrombin-induced permeability (data not shown). The bio-ligands for cAMP-elevating GPCR that we used in this study indeed increased cAMP in HUVECs (data not shown). Furthermore, IBMX (an inhibitor for phosphodiesterase), dbcAMP (a membrane-permeable cAMP analogue), and FSK (an adenylyl cyclase activator) resulted in a reduction of both basal and thrombin-induced endothelial permeability (Fig. 1; data not shown).

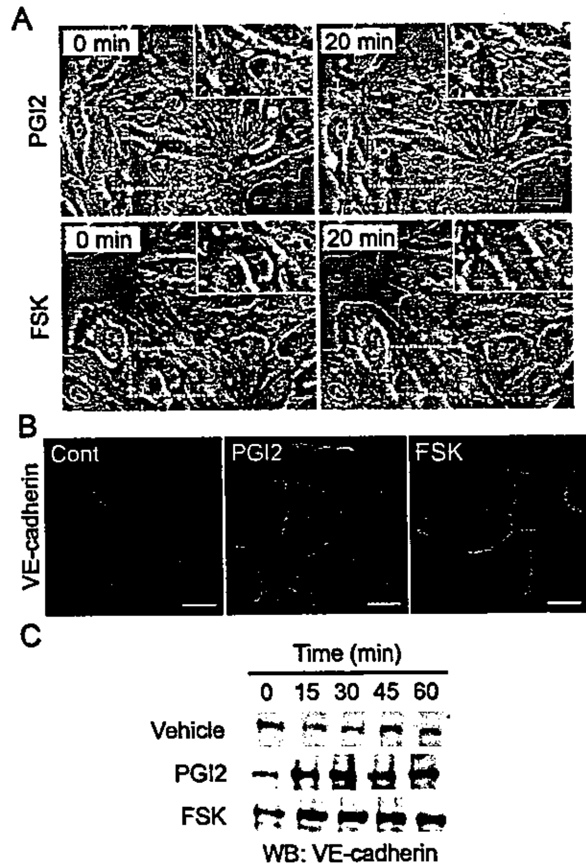

FIG. 2. cAMP induces AJ formation. (A) HUVECs cultured on a glass base dish were stimulated with 10 μg of PGI2/ml (upper panels) or with 10 μM FSK (lower panels) for 20 min and shown as phase-contrast images. Left and right panels show the cells before and after stimulation, respectively. The arrows indicate the sites of cell-cell contacts induced by PGI2 and FSK. The area boxed by the white broken line is enlarged in the right top of the panels. Bars, 50 μm. (B) Subconfluent HUVECs stimulated with vehicle (Cont), 10-μg/ml PGI2, and 10 μM FSK for 45 min were fixed, stained with anti-VE-cadherin antibody, and visualized with Alexa 488-conjugated secondary antibody through a confocal microscope (BX50WI; Olympus). Note that VE-cadherin (green) was accumulated at the cell-cell contact upon PGI2 and FSK stimulation. Bars, 50 μm. (C) Translocation of VE-cadherin was assessed by Triton X-100 solubility. HUVECs were stimulated with vehicle (top), 10-μg/ml PGI2 (middle), and 10 μM FSK (bottom) for the time indicated at the top and fractionated with cytoskeleton-stabilizing buffer as described in Materials and Methods. The Triton X-100-insoluble fraction was subjected to SDS-PAGE followed by Western blot analysis (WB) with anti-VE-cadherin.

cAMP potentiates formation of AJ. Endothelial barrier function is largely dependent upon endothelial cell junctions. To investigate how cAMP affects AJ formation, we examined AJ organization by immunostaining with anti-VE-cadherin before and after stimulation. When subconfluent HUVECs with intercellular gaps were stimulated with PGI2 or FSK, the cells extended the plasma membrane and established cell-cell contacts with neighboring cells (Fig. 2A). Similar results were

obtained with AM and PGE2 (data not shown). Stimulation of HUVECs with PGI2 and FSK dramatically enhanced accumulation of VE-cadherin at cell-cell contacts (Fig. 2B).

The maturation of AJ requires homophilic binding of intercellular VE-cadherins and tight anchoring to the actin cytoskeleton via the cytoplasmic region through catenins. VE-cadherin anchored to the actin cytoskeleton is detected in detergent-insoluble fractions of cell lysates (26). We found an increase in VE-cadherin in the Triton X-100-insoluble fraction after stimulation with PGI2 or FSK (Fig. 2C). These results suggest that cAMP-elevating GPCR agonists potentiate AJ formation, which results in a cAMP-induced decrease in permeability.

cAMP promotes VE-cadherin-dependent endothelial cell adhesion. VE-cadherin is required for AJ formation (9). To test the involvement of a homophilic interaction of VE-cadherin in cAMP-enhanced AJ formation, we directly examined VE-cadherin-mediated cell adhesion. To mimic the VE-cadherin-dependent cell adhesion, we used VEC-Fc chimeric protein, which consisted of the extracellular domain of VE-cadherin fused to the Fc portion of immunoglobulin. HUVECs were plated onto VEC-Fc-coated dishes and time-lapse imaged. Cells attached within 5 min to the VEC-Fc-coated dish, subsequently spread, and exhibited a typical fried-egg morphology characterized by a large circular lamellipodium (Fig. 3A). No cells attached to the Fc-coated dish (Fig. 3B and C). Since cadherin-dependent cell adhesion requires Ca^{2+}, we examined the effect of Ca^{2+} chelation on cell adhesion to VEC-Fc-coated dishes. Cell adhesion to VEC-Fc-coated dishes was completely abolished by chelating extracellular Ca^{2+}, although cell attachment to the collagen-coated dish was unaffected (Fig. 3C and D). Basal and FSK-augmented cell adhesion to VEC-Fc-coated dishes was inhibited by EGTA (Fig. 3C). Both HUVECs and HAECs expressing VE-cadherin adhered to the VEC-Fc-coated dish (Fig. 3E). In clear contrast, HeLa and HEK293 cells, which express N-cadherin, but not VE-cadherin (20, 42), did not adhere to the VEC-Fc-coated dish, although these cells could attach to the collagen-coated dish (Fig. 3E; data not shown). Collectively, these results indicate that endothelial cell adhesion to the VEC-Fc-coated dish depends upon the homophilic ligation of VE-cadherin.

We proceeded to investigate the effect of cAMP-elevating GPCR agonists on VE-cadherin-mediated cell adhesion. The adhesion of HUVECs plated in the presence of PGI2 or FSK was evaluated by the alkaline phosphatase activity of remaining cells after washing. PGI2 enhanced adhesion of HUVECs to the VEC-Fc-coated dish in a concentration-dependent manner (Fig. 4A) and in a time-dependent manner (Fig. 4B). In a time course analysis, we noticed that enhanced adhesion was observed 7 min after the plating (Fig. 4B). Other cAMP-elevating GPCR agonists, including AM, Iso, and PGE2, potentiated VE-cadherin-dependent cell adhesion (Fig. 4C). In addition, similarly enhanced cell adhesion to the VEC-Fc-coated dish was also observed in the cells treated with cAMP-elevating drugs such as IBMX, dbcAMP, and FSK (Fig. 4F). Like PGI2, the effect of FSK on cell adhesion to the VEC-Fc-coated dish was concentration dependent and time dependent (Fig. 4D and E). This cAMP-induced cell adhesion to the VEC-Fc-coated dish depends on the enhanced homophilic ligation of VE-cadherin because FSK did not augment endothelial adhe-

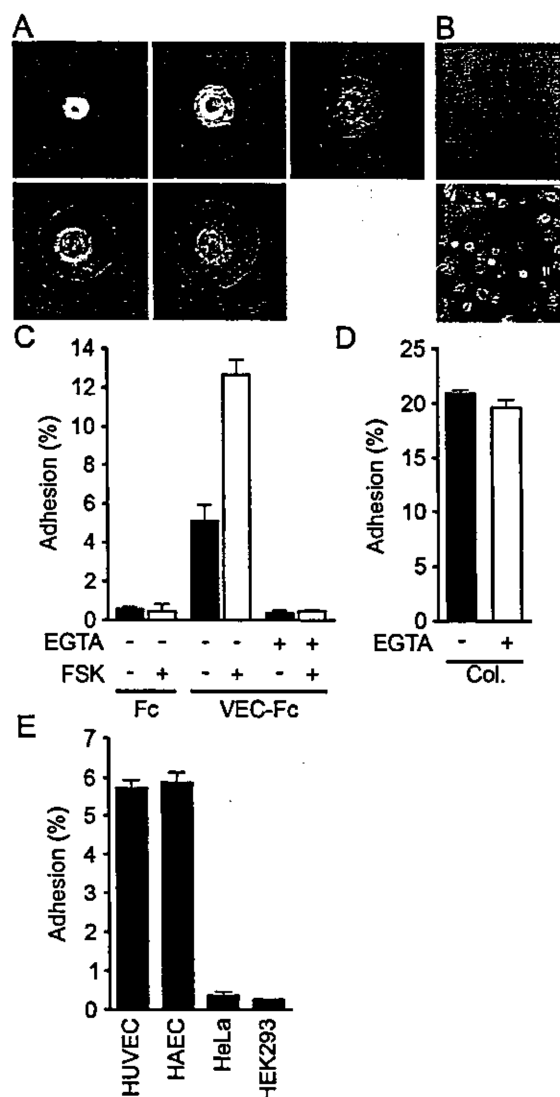

FIG. 3. Endothelial cells adhere to a VEC-Fc-coated dish through homophilic ligation of VE-cadherin. (A) HUVECs were plated onto the VEC-Fc-coated dish and time-lapse imaged at the time points (in minutes) indicated on the panels. Bar, 20 μM. (B) HUVECs were plated on the Fc-coated dish (top panel) or the VEC-Fc-coated dish (bottom panel) for 1 h and phase-contrast imaged after removal of nonadherent cells by washing with PBS-Ca/Mg. (C) HUVECs were plated onto either an Fc- or VEC-Fc-coated dish in the absence (−) or presence (+) of 5 mM EGTA and 10 μM FSK for 7 min. Cell adhesion was quantified as described in Materials and Methods. (D) Adhesion of HUVECs to a collagen-coated dish in the presence or absence of 5 mM EGTA was analyzed by a method similar to that described for panel C. (E) Adhesion of HUVECs, HAECs, and HeLa and HEK293 cells to the VEC-Fc-coated dish was examined as described in the legend for panel C. Cells adhering to the dishes of total input cells (percentage) is expressed as the mean ± standard deviation by measuring alkaline phosphatase activity of adherent cells divided by that of total input cells. Representative results from three independent experiments were shown in all panels.

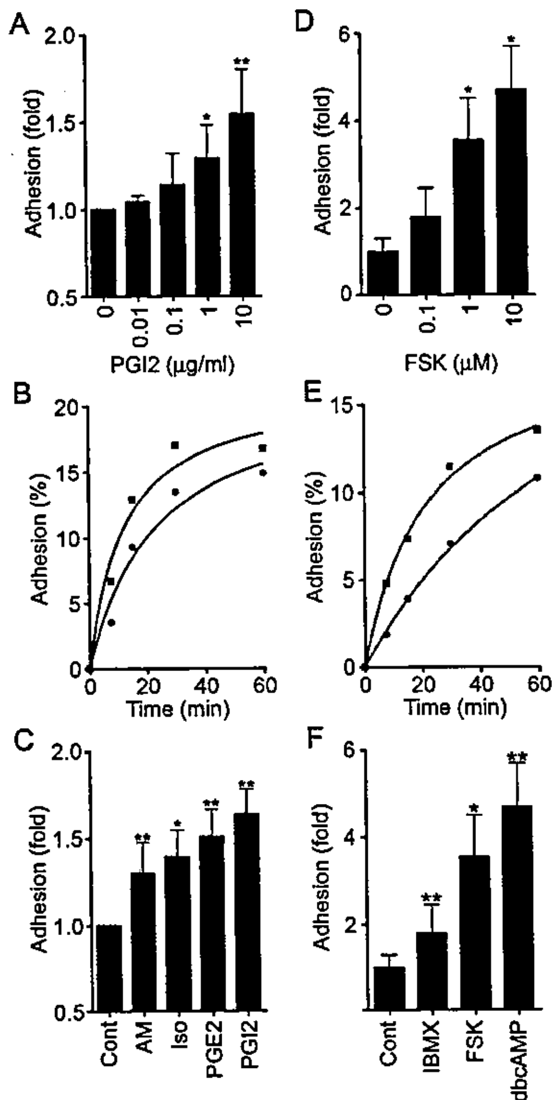

FIG. 4. cAMP potentiates VE-cadherin-dependent cell adhesion. (A) HUVECs were plated onto a VEC-Fc-coated dish in the presence of PGI2 at the concentrations indicated at the bottom for 7 min. Cell adhesion was quantified as described in Materials and Methods. Mean adhesion activity ± standard deviation is expressed as the increase compared with that observed in unstimulated cells. (B) HUVECs were plated onto the VEC-Fc-coated dish in the absence (circle) or presence (square) of 10-μg/ml PGI2 for the time indicated at the bottom. The percent adhesion was calculated by measuring the alkaline phosphatase activity of adherent cells divided by that of total input cells. (C) HUVECs stimulated with cAMP-elevating ligands similar to that described in the legend to panel A were assessed for adhesion activity. The concentration of stimulants was the same as described in the legend to Fig. 1A. (D) The effect of FSK on cell adhesion was analyzed by a method similar to that described for panel A, except that cells were preincubated for 10 min before plating. (E) The effect of 10 μM FSK on time-dependent adhesion was analyzed as described in the legend to panel B, except that cells were preincubated for 10 min before plating. (F) HUVECs stimulated with the reagent indicated at the same concentration used as described in the legend to Fig. 1A were analyzed for cell adhesion by a method similar to that described for panel D. Data are expressed as means ± standard deviations of the results from three independent experiments in panels A, C, D, and F. Representative results from three independent experiments were shown in panels B and E. A significant difference from the control determined by Student's *t* test is indicated with a single asterisk ($P < 0.05$) or double asterisks ($P < 0.01$).

sion to the Fc-coated dish or attachment to the VEC-Fc-coated dish in the absence of extracellular Ca^{2+} (Fig. 3C). These results indicate that cAMP potentiates VE-cadherin-dependent cell adhesion.

cAMP augments endothelial barrier function in a PKA-independent manner. PKA is suggested to be involved in cAMP-enhanced endothelial barrier function (43). Thus, we investigated the involvement of PKA in the regulation of endothelial barrier integrity by PGI2 and FSK. Unexpectedly, PGI2- and FSK-induced reduction of endothelial permeability was insensitive to a specific PKA inhibitor, H89 (7) (Fig. 5A and B). The reduction of thrombin-increased permeability by FSK was also unaffected by H89 (Fig. 5C). Consistently, H89 did not affect VE-cadherin-mediated cell adhesion enhancement by PGI2 and FSK (Fig. 5D and E). To confirm that H89 worked in HUVECs, we examined FSK-induced phosphorylation of CREB, a direct PKA substrate (38). Phosphorylation of CREB upon FSK stimulation was significantly inhibited by H89, indicating the effectiveness of this inhibitor in HUVECs (Fig. 5F). Therefore, these results apparently suggest a novel PKA-independent signaling pathway involved in cAMP-induced endothelial barrier function.

cAMP induces Rap1 activation. Besides PKA, Epac (cAMP-GEF) was identified as a novel cAMP target and a Rap1-specific GEF (5, 21). We therefore hypothesized that cAMP-activated Epac-Rap1 signaling is involved in the enhancement of VE-cadherin-dependent cell adhesion and endothelial barrier function. To address this possibility, we tested whether cAMP-elevating GPCR agonists induce Rap1 activation in HUVECs. Rap1 activity was determined by a pull-down assay by using a GST fusion protein of Rap1-binding domain of RalGDS according to the Bos's method. Bio-ligands for cAMP-elevating GPCR activated Rap1 (Fig. 6A). PGI2 rapidly induced Rap1 activation, which peaked at 1 to 5 min after the stimulation and then declined to the basal level by 10 min (Fig. 6C). A second wave of Rap1 activation was also observed 15 to 45 min after the stimulation (Fig. 6C). PGI2-induced Rap1 activation occurred in a concentration-dependent manner (Fig. 6B), which was associated with enhancement of VE-cadherin-dependent cell adhesion (Fig. 4A). Similarly, dbcAMP, FSK, and IBMX activated Rap1 (Fig. 6D). FSK-induced Rap1 activation reached a maximal level 2 to 5 min after the stimulation, and the level was sustained for up to 15 to 30 min (Fig. 6E). Collectively, these findings indicate that cAMP induces Rap1 activation in endothelial cells.

Specific activation of Epac reduces endothelial permeability and enhances VE-cadherin-dependent cell adhesion. To test whether the activation of endogenous Epac is sufficient to reduce endothelial permeability and to induce VE-cadherin-dependent cell adhesion, we used a recently developed cAMP analog, 8-CPT-2′-O-Me-cAMP, which specifically activates Epac without affecting PKA activity (13). As expected, 8-CPT-2′-O-Me-cAMP induced Rap1 activation in HUVECs (Fig. 7A), indicating that Epac is expressed in endothelial cells.

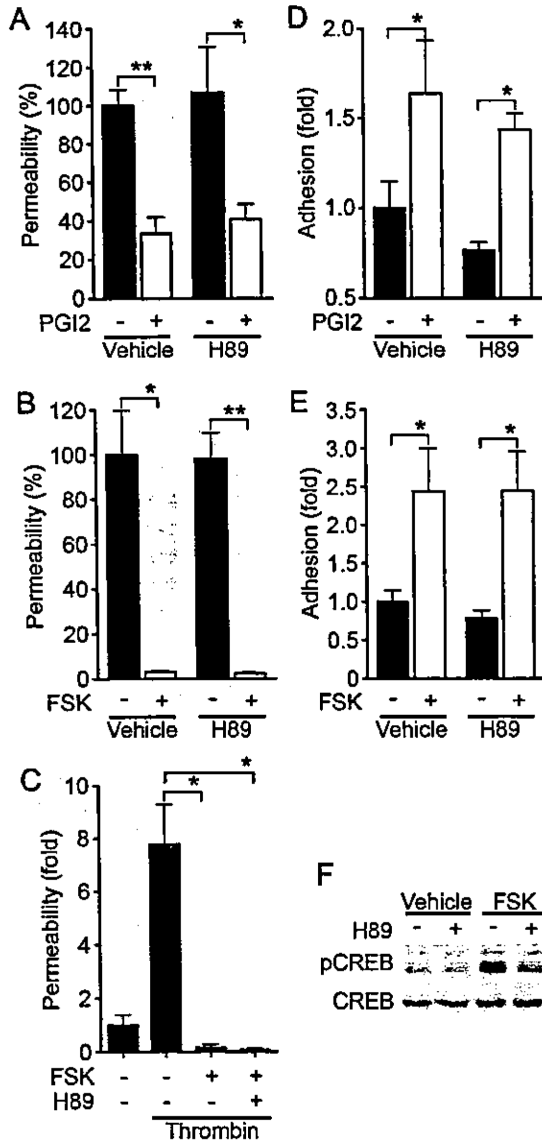

FIG. 5. cAMP-enhanced VE-cadherin-dependent cell adhesion and endothelial barrier function does not depend upon PKA. (A) Permeability across monolayer HUVECs grown on transwell filters were assessed by measuring FITC-labeled dextran as described in the legend to Fig. 1A. The effect of 10-μg/ml PGI2 on cell permeability without pretreatment (Vehicle) or with pretreatment with 5 μM H89, a specific PKA inhibitor, for 10 min is indicated as the percent permeability compared to that observed in untreated cells. +, present; −, absent. (B) The effect of 10 μM FSK on cell permeability without pretreatment (Vehicle) and with pretreatment with H89 was assessed similar to that described for panel A. (C) The effect of pretreatment of HUVECs with 5 μM H89 on FSK-induced reduction of 2-U/ml thrombin-induced permeability was analyzed. Permeability indicates the increase relative to that observed in untreated cells. (D) HUVECs untreated or pretreated with H89 for 10 min prior to stimulation with 10-μg/ml PGI2 were analyzed for cell adhesion as described in the legend to Fig. 4A. (E) HUVECs untreated or pretreated with H89 for 10 min prior to stimulation with 10 μM FSK were analyzed for cell adhesion as described in the legend to Fig. 4D. For panels A to E, data are expressed as means ± standard deviations of the results from triplicate samples. Similar results were obtained in at least three independent experiments. Significant differences between two groups determined by Student's t test are indicated by a single asterisk ($P < 0.05$) or double asterisks ($P < 0.01$). (F) HUVECs serum starved in 1% BSA-containing medium 199 for 6 h, followed by pretreatment with (+) or without (−) 5 μM H89 for 10 min, were stimulated with vehicle and 10 μM FSK for 10 min. Phosphorylation of CREB was assessed by Western blot analysis with anti-CREB (CREB) and anti-phospho-CREB-specific (pCREB) antibodies.

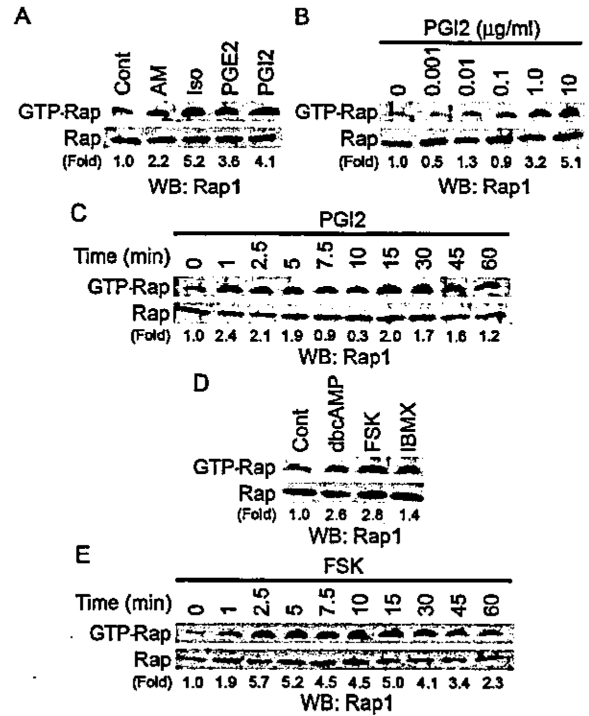

FIG. 6. cAMP induces Rap1 activation. (A) Serum-starved HUVECs kept in medium 199 containing 1% BSA overnight were stimulated with cAMP-elevating agonists for 2.5 min as indicated at the top and at the concentrations described in the legend to Fig. 1A. GTP-bound Rap1 was detected by pull-down assay as described in Materials and Methods. Activation indicates the ratio of the poststimulation GTP-Rap1 intensity of total Rap1 intensity to the prestimulation GTP-Rap1 intensity of total Rap1 intensity. (B) Rap1 activation was analyzed by detecting GTP-bound Rap1 with lysates from HUVECs stimulated with PGI2 for 2.5 min at the different concentrations indicated at the top. (C) Rap1 activation was analyzed by detecting GTP-bound Rap1 with lysates from cells stimulated with 10-μg/ml PGI2 for the time period indicated at the top. (D) Serum-starved HUVECs similar to those described in the legend to panel A were stimulated with the reagents indicated at the top for 10 min at the same concentrations described in the legend to Fig. 1A. Rap1 activation was assessed by a method similar to that described for panel A. (E) The effect of 10 μM FSK on time-dependent Rap1 activity was examined as described for panel C. Representative results from at least three independent experiments are shown for all panels.

8-CPT-2′-O-Me-cAMP dramatically reduced basal endothelial permeability, as did FSK and dbcAMP (Fig. 7B). Thrombin-induced permeability was also inhibited by 8-CPT-2′-O-Me-cAMP (Fig. 7C). Furthermore, we examined the effect of 8-CPT-2′-Me-cAMP on in vivo vascular permeability. VEGF-induced vascular permeability was completely blocked by coinjection of 8-CPT-2′-O-Me-cAMP (Fig. 7D). In addition, adhesion

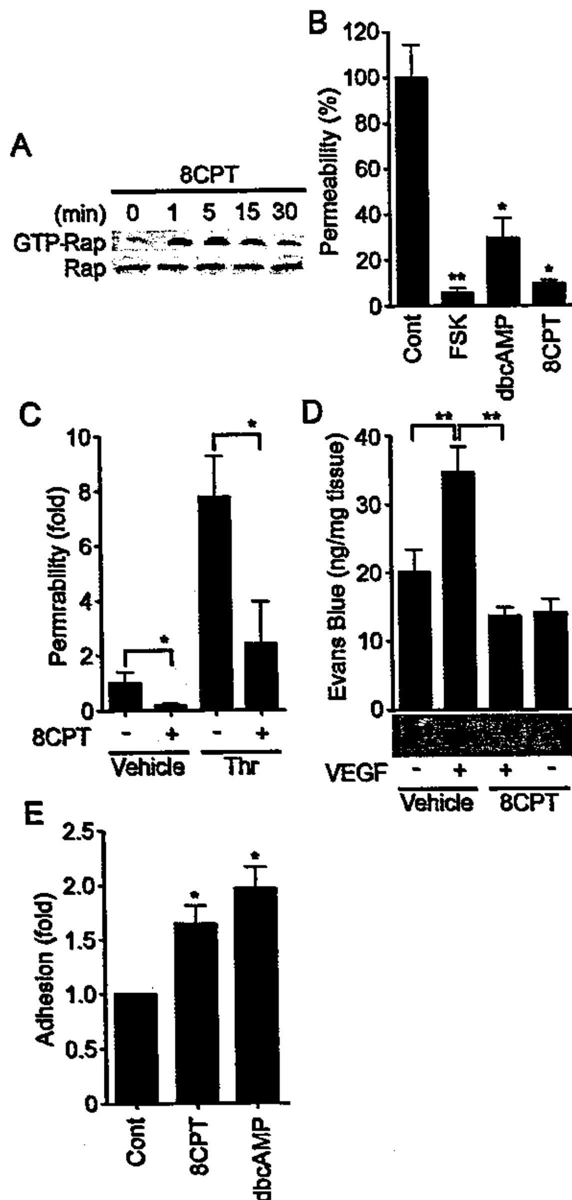

FIG. 7. Activation of Epac is sufficient to enhance VE-cadherin-dependent cell adhesion and endothelial barrier function. (A) Serum-starved HUVECs in medium 199 containing 1% BSA were stimulated with 0.2 mM 8-CPT-2′-O-Me-cAMP (8CPT) for the indicated time. Rap1 activity was determined as described in the legend to Fig. 6A. The result is a representative from three independent experiments. (B) Permeability of cells treated with the reagents as indicated on the bottom for 30 min was analyzed as described in the legend to Fig. 1A. (C) The effect of 0.2 mM 8CPT-2′-O-Me-cAMP on 2-U/ml thrombin-induced permeability was analyzed as described in the legend to Fig. 1B. (D) Effect of 8CPT-2′-O-Me-cAMP on VEGF-induced permeability was assessed by intradermal Miles assay as described in Materials and Methods. Amounts of extravasation of Evan blue in mouse dermal skin were measured 60 min after intradermal injection of vehicle and VEGF together with (+) or without (−) 8CPT. Mean leakage ± standard deviation of the results from 6 mice per group is expressed as nanograms of weight of extravasated Evans blue per milligram of weight of dermal skin. A photograph on the bottom shows leakage of Evans blue in dermal skin. (E) HUVEC adhesion to the VEC-Fc-coated dish in the presence of 0.2 mM 8CPT and 1 mM dbcAMP for 7 min was analyzed as described in the legend to Fig. 4F. In panels B, C, and E, data are expressed as means ± standard deviations of the results from triplicate samples. A significant difference from the control in panels B and E or between two groups in panels C and D was determined by Student's t test and indicated by a single asterisk ($P < 0.05$) or double asterisks ($P < 0.01$).

of HUVECs to the VEC-Fc-coated dish was significantly enhanced by 8-CPT-2′-O-Me-cAMP (Fig. 7E). Hence, Epac activation is sufficient to enhance VE-cadherin-dependent cell adhesion and to augment endothelial barrier function in vitro and in vivo.

Rap1 activation is essential for VE-cadherin-dependent cell adhesion and endothelial barrier function. We next proceeded to investigate the role of Rap1 in VE-cadherin-dependent cell adhesion and endothelial barrier function. To examine the effect of Rap1 on cell permeability and VE-cadherin-mediated cell adhesion, we inactivated endogenous Rap1 by adenovirus-expressing Rap1GAPII (Ad-RapGAP), which specifically catalyzes the hydrolysis of GTP to GDP on Rap1 (30). As shown in Fig. 8A, endogenous Rap1 activity was almost completely suppressed by the expression of increasing amounts of Rap1GAPII in HUVECs. This Rap1 inactivation paralleled the increase in basal permeability (Fig. 8B) and the inhibition of cell adhesion to the VEC-Fc-coated dish (Fig. 8D). In contrast, a constitutively active Rap1, Rap1V12, reduced both basal and thrombin-increased cell permeability (Fig. 8C). VE-cadherin-mediated cell adhesion was also enhanced by Rap1V12 and EpacΔcAMP, a constitutively active mutant of Epac (Fig. 8D). Taken together, these results indicate that Rap1 activation is required for VE-cadherin-mediated cell adhesion and endothelial barrier function.

cAMP enhances VE-cadherin-dependent cell adhesion and endothelial barrier function by activating Rap1. To test the requirement for Rap1 in endothelial barrier enhancement by cAMP-elevating GPCR agonists, we infected HUVECs with Ad-RapGAP and examined the effect of inactivation of Rap1 on PGI2- and FSK-induced reduction of cell permeability. Although basal endothelial permeability was reduced by PGI2 and FSK (Fig. 9A and B), overexpression of Rap1GAPII increased not only basal but also PGI2- and FSK-reduced endothelial permeability, indicating the requirement of Rap1 activity for PGI2- and FSK-induced barrier enhancement. We also investigated the involvement of Rap1 in PGI2- and FSK-induced VE-cadherin-dependent cell adhesion. PGI2 and FSK augmented VE-cadherin-dependent cell adhesion of HUVECs infected with control adenovirus (Ad-LacZ); however, their effects were dramatically suppressed by overexpression of Rap1GAPII (Fig. 9C and D). These data demonstrate that cAMP enhances VE-cadherin-dependent cell adhesion and endothelial barrier functions by activating Rap1.

cAMP induces endothelial cortical actin rearrangement in a Rap1-dependent manner. Endothelial barrier function is largely dependent upon the actin cytoskeleton supporting junctional adhesion molecules (10). Thus, we examined the effect of cAMP on cortical actin polymerization and assembly of polymerized actin in a monolayer of endothelial cells. Cortactin, an actin-binding protein, is known to be implicated in cortical actin rearrangement (8) and suggested to regulate S1P-induced endothelial barrier enhancement (11). PGI2,

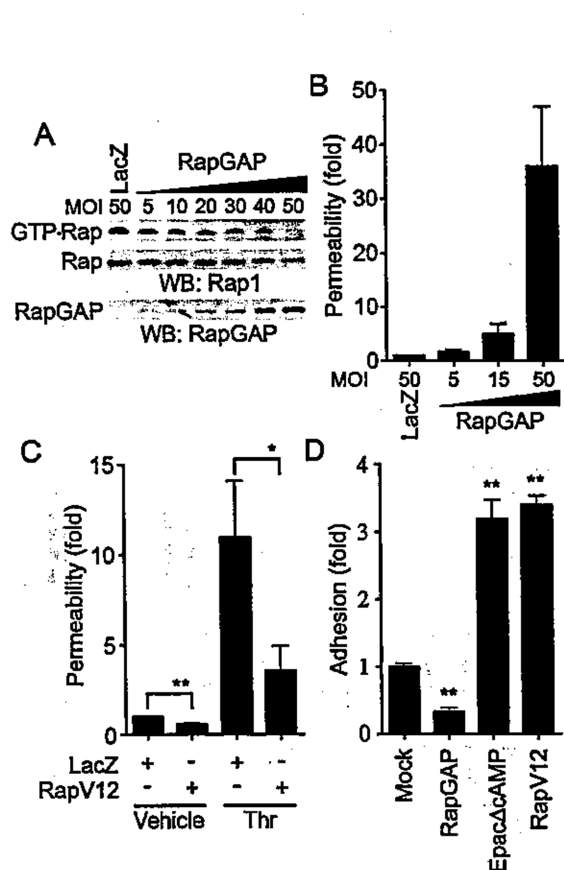

FIG. 8. Rap1 plays a critical role in VE-cadherin-dependent cell adhesion and endothelial barrier function. (A) Rap1 inactivation was assessed by detecting GTP-Rap1 in HUVECs infected with different MOI of adenovirus-expressing Rap1GAPII (RapGAP) as indicated at the top. An adenovirus-expressing LacZ at an MOI of 50 was used as a control. GTP-bound Rap1 (GTP-Rap) was detected by pull-down assay as described in Materials and Methods. Rap1 (Rap) and Rap1GAPII (RapGAP) expression were examined by Western blot analysis. (B) The permeability of FITC-dextran across HUVECs infected with adenovirus as indicated at the bottom was analyzed as described in Materials and Methods. Data are the means ± standard deviations of the results from three independent experiments and are expressed as increases relative to those of LacZ-infected cells. (C) Monolayer HUVECs infected with either an adenovirus-expressing LacZ or that expressing Rap1V12 at an MOI of 50 for 24 h were medium changed and cultured for another 24 h. The permeability of cells upon 2-U/ml thrombin stimulation (Thr) after starvation for 1 h was analyzed as described in the legend to Fig. 1B. Data are the means ± standard deviations of the results from five independent experiments and are expressed as inductions relative to those of untreated HUVECs infected with the LacZ-expressing virus. (D) HUVECs were transfected with either empty vector (Mock), plasmids expressing Rap1GAPII (RapGAP), EpacΔcAMP, or Rap1V12 together with the luciferase reporter construct. Transfected cells were plated on the VEC-Fc-coated dish and allowed to adhere for 15 min. Cell adhesion was analyzed as described in Materials and Methods. Data are expressed as increases compared to those of mock-transfected cells. The results indicate the means ± standard deviations of the results from triplicate samples. Similar results were obtained in three independent experiments. Significant differences between two groups in panel C or from the control in panel D are determined by Student's t test and are indicated by a single asterisk ($P < 0.05$) or double asterisks ($P < 0.01$).

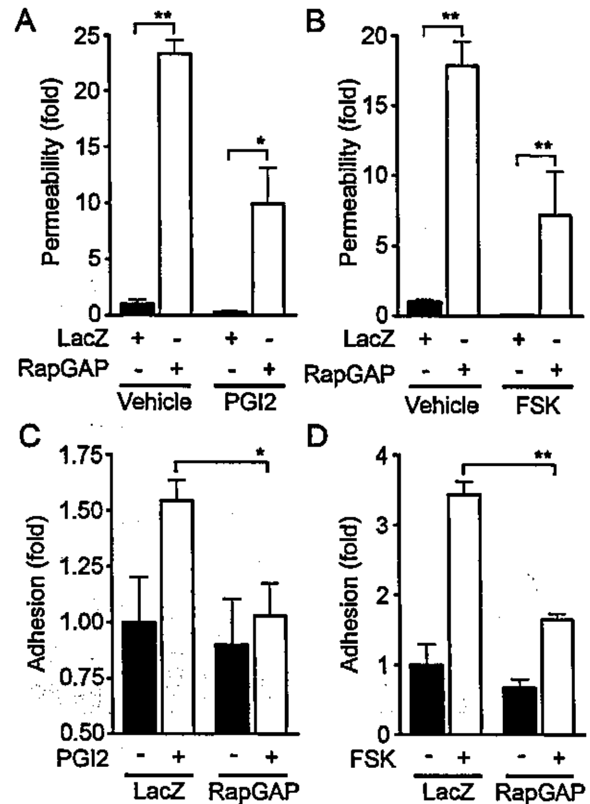

FIG. 9. Inactivation of Rap1 reduces PGI2- and FSK-induced barrier function and VE-cadherin-mediated cell adhesion. (A) Monolayer-cultured HUVECs grown on transwell filters were infected with either LacZ-expressing adenovirus (Ad-LacZ) or Rap1GAPII-expressing virus (Ad-RapGAP) at an MOI of 40 for 24 h. Medium was replaced with fresh medium after infection. Cells were cultured for an additional 24 h and treated with 10 μg of PGI2/ml for 30 min after serum starvation for 1 h. Permeability was analyzed as described in Materials and Methods. (B) The effect of 10 μM FSK on permeability in HUVECs infected with Ad-RapGAP was similarly analyzed. (C) HUVECs were infected with either Ad-LacZ or Ad-RapGAP at an MOI of 40 for 24 h. HUVECs resuspended in medium 199 with 0.5% BSA were plated onto VEC-Fc-coated dishes in the presence (+) or absence (−) of 10 μg of PGI2/ml for 7 min. Cell adhesion activity was quantified as described in the legend to Fig. 4A. (D) The effect of FSK on adhesion of HUVECs infected with Ad-RapGAP was analyzed similarly to that described for panel C. Resuspended HUVECs were preincubated with 10 μM FSK for 10 min before plating. Significant differences between two groups determined by Student's t test are indicated by a single asterisk ($P < 0.05$) or double asterisks ($P < 0.01$).

FSK, and 8-CPT-2′-O-Me-cAMP dramatically induced accumulation of polymerized actin and cortactin at cell-cell contacts (Fig. 10A). To explore the involvement of Rap1 in cAMP-mediated cortical actin rearrangement, an expression vector encoding Rap1GAPII was introduced into endothelial cells. FSK enhanced actin polymerization at cell-cell contacts in cells transfected with control vector encoding EGFP, whereas it did not in cells expressing Rap1GAPII (Fig. 10B). Cytochalasin D, an actin-depolymerizing agent, attenuated FSK-induced barrier enhancement (Fig. 10C) and inhibited FSK-induced VE-cadherin-dependent cell adhesion (Fig. 10D). These results suggest that the cortical actin rearrangement promoted by

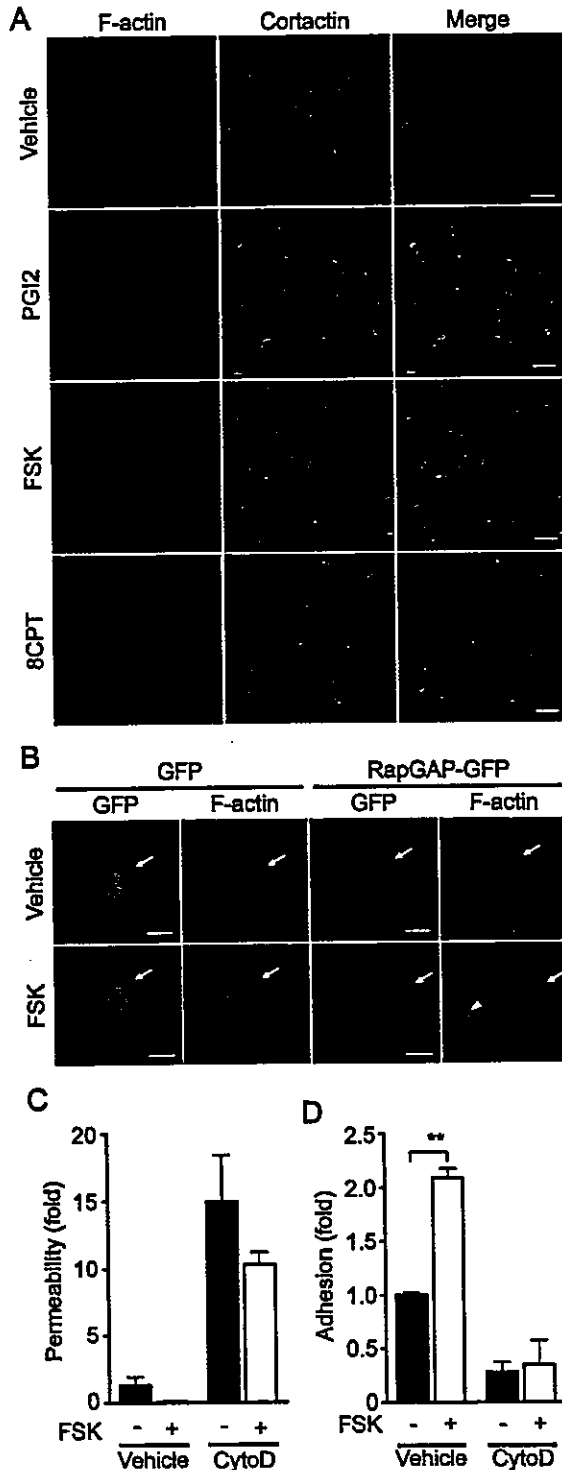

FIG. 10. cAMP induces cortical actin rearrangement in a Rap1-dependent manner. (A) Monolayer-cultured HUVECs starved in 0.5% BSA-containing medium 199 for 3 h were stimulated with vehicle (top row), 10-μg/ml PGI2 (second row), 10 μM FSK (third row), and 0.2 mM 8-CPT-2′-O-Me-cAMP (8CPT) (bottom row) for 30 min. Fixed and permeabilized cells were stained with rhodamine-phalloidin (left column) and with anti-cortactin (center column). Rhodamine images to detect F-actin (red) and Alexa 488 images for cortactin visualized by Alexa 488-labeled secondary antibody (green) were obtained through a confocal microscope (BX50WI). Right panels show the merged images of rhodamine and Alexa 488 images. Bars, 20 μm. (B) HUVECs transfected with an EGFP-expressing vector (left) and pCXN2-Rap1GAPII-IRES-EGFP (right) were serum starved in 0.5% BSA-containing medium 199 for 3 h and stimulated with vehicle (top panels) and 10 μM FSK (bottom panels). Cells were fixed, permeabilized, and stained with Rhodamine-phalloidin. EGFP images (green) and rhodamine images showing F-actin (red) were obtained similar to those in panel A. Arrows and arrowhead indicate transfected and untransfected cells, respectively. Bars, 20 μm. (C) Cell permeability of HUVECs pretreated with 2 μM cytochalasin D (CytoD) for 30 min followed by 10 μM FSK stimulation for 30 min was analyzed as described in the legend to Fig. 1A. −, absent; +, present. (D) The effect of pretreatment of 2 μM cytochalasin D (CytoD) on adhesion of HUVECs stimulated with FSK was analyzed as described in the legend to Fig. 5E. A significant difference between two groups determined by Student's t test is indicated by double asterisks ($P < 0.01$).

cAMP-Epac-Rap1 signaling may contribute to the potentiation of endothelial barrier function and VE-cadherin-dependent cell adhesion.

DISCUSSION

cAMP is a well-known intracellular signaling molecule that is capable of restoring diminished endothelial barrier function. Previous reports suggested that cAMP-induced barrier enhancement occurs through PKA (27, 39). In this study, however, we demonstrated a novel PKA-independent signaling pathway, the cAMP-Epac-Rap1 signaling pathway, involved in cAMP-induced barrier function based on the following observations. PGI2- and FSK-reduced endothelial permeability was insensitive to H89. A specific activator for Epac, 8-CPT-2′-O-Me-cAMP, reduced both basal and thrombin-increased permeability. Plasma leakage in response to VEGF was also inhibited by 8-CPT-2′-O-Me-cAMP in vivo. We found that the activation of Rap1 leads to decreased permeability. Not only all cAMP-elevating bio-ligands we tested but also FSK, db-cAMP, and IBMX activated Rap1. Consistently, cAMP-dependent Rap1 activation upon stimulation by these ligands involved Epac in the regulation of barrier function. A previous report showed that Rap1 is phosphorylated by PKA in neutrophils and platelets, although the function of phosphorylated Rap1 has not been elucidated (37). So far, Epac is known to regulate several biological functions including integrin-dependent cell adhesion, insulin secretion, and calcium release through ryanodine-sensitive Ca^{2+} channels (reviewed in reference 5). In addition to these Epac-mediated functions, we show, for the first time, that Epac-Rap1 signaling is important for regulation of endothelial barrier function.

AJ assembly contributes to the regulation of barrier function. Rap1 is involved in the formation and maintenance of AJ constituted by cadherin (23, 41). Recently, it has been reported that homophilic ligation of E-cadherin induced Rap1 activation, which may be responsible for maturation of AJ (20). Consistently, suppression of endogenous Rap1 inhibits formation of E-cadherin-dependent cell adhesion (36), suggesting the critical role of Rap1 in the establishment of cadherin-based cell-cell contacts. Here, we demonstrate that Rap1 also acts downstream of cAMP-Epac to potentiate VE-cadherin-depen-

dent cell adhesion, thereby improving barrier function. In addition to cAMP-elevating ligands, S1P, which enhances AJ formation and barrier function (18, 26), also activated Rap1 (our unpublished data). Thus, Rap1 may play a crucial role in barrier function induced by various types of barrier-improving factors.

Our data and previous studies show that cAMP protects thrombin-induced endothelial barrier dysfunction. cAMP does not limit the effect of thrombin on the initial loss of endothelial barrier (32). Instead, cAMP enhances the restoration of barrier function disrupted by thrombin. Recently, it was also reported that Cdc42 regulates the restoration of endothelial barrier function disrupted by thrombin (24). Thus, cAMP-Epac-Rap1 signaling may facilitate the formation of VE-cadherin-based cell-cell contacts, cooperatively or in parallel with Cdc42.

Rap1 enhances integrin-dependent cell adhesion in a variety of hematopoietic cells by modulating the affinity and avidity of integrin (6, 22). Cell adhesion to VEC-Fc-coated dishes was augmented by Rap1 activation, suggesting that the homophilic binding of VE-cadherin is also likely ascribed to the affinity and avidity of VE-cadherin modulated by Rap1-triggered inside out signaling. Hogan et al. reported that Rap1 activity is required for the targeting of E-cadherin molecules into nascent cell-cell contact sites, which in turn leads to the maturation of E-cadherin-based cell-cell contacts (20). Thus, cAMP-Epac-Rap1 signaling may also regulate the recruitment of VE-cadherin into maturing cell-cell contacts. Since downstream signaling of Rap1 that increases homophilic binding of VE-cadherin has not yet been characterized, the effector of cAMP-Epac-Rap1 signaling will need to be identified.

The actin cytoskeleton is a critical determinant of vascular integrity (10). PGI2, FSK, and 8-CPT-2'-O-Me-cAMP induced cortical actin rearrangement in a Rap1-dependent manner. FSK-induced VE-cadherin-dependent cell adhesion was inhibited by cytochalasin D. Thus, Rap1 may promote VE-cadherin-dependent cell adhesion by inducing cortical actin rearrangement. AF-6 may act downstream of Rap1 to regulate the actin cytoskeleton, since it binds to GTP-bound Rap1 and the actin cytoskeleton regulator, profilin, and is localized at AJ (2). Consistently, Canoe, the drosophila homolog of AF-6, and Rap1 function in the same molecular pathway during embryonic dorsal closure, which requires cell-cell contacts (3). S1P promotes endothelial barrier function by inducing Rac-dependent cortical actin rearrangement. S1P also induces Rap1 activation (our unpublished data). A previous report indicates that Rac can function downstream of Rap1 in the processing of the amyloid precursor protein (28). Taken together, Rac may act downstream of Rap1 to induce cortical actin rearrangement.

In conclusion, we have demonstrated that the cAMP-Epac-Rap1 signaling pathway promotes VE-cadherin-mediated cell adhesion and consequently improves endothelial barrier function.

ACKNOWLEDGMENTS

We thank J. L. Bos and W. A. Muller for plasmids, M. Matsuda and S. Hattori for adenovirus, J. T. Pearson for critical reading, and M. Sone, K. Yamamoto, and N. Irisawa for technical assistance.

This work was supported by grants from the Ministry of Health, Labor, and Welfare of Japan, from the Promotion of Fundamental Studies in Health Science of the Organization for Pharmaceutical Safety and Research of Japan, from the Ministry of Education, Science, Sports, and Culture of Japan, from the Uehara Memorial Foundation, and from Senri Life Science Foundation.

REFERENCES

1. **Andriopoulou, P., P. Navarro, A. Zanetti, M. G. Lampugnani, and E. Dejana.** 1999. Histamine induces tyrosine phosphorylation of endothelial cell-to-cell adherens junctions. Arterioscler. Thromb. Vasc. Biol. 19:2286–2297.
2. **Boettner, B., E. E. Govek, J. Cross, and L. Van Aelst.** 2000. The junctional multidomain protein AF-6 is a binding partner of the Rap1A GTPase and associates with the actin cytoskeletal regulator profilin. Proc. Natl. Acad. Sci. USA 97:9064–9069.
3. **Boettner, B., P. Harjes, S. Ishimaru, M. Heke, H. Q. Fan, Y. Qin, L. Van Aelst, and U. Gaul.** 2003. The AF-6 homolog canoe acts as a Rap1 effector during dorsal closure of the Drosophila embryo. Genetics 165:159–169.
4. **Bogatcheva, N. V., J. G. Garcia, and A. D. Verin.** 2002. Molecular mechanisms of thrombin-induced endothelial cell permeability. Biochemistry (Moscow) 67:75–84.
5. **Bos, J. L.** 2003. Epac: a new cAMP target and new avenues in cAMP research. Nat. Rev. Mol. Cell Biol. 4:733–738.
6. **Bos, J. L., J. de Rooij, and K. A. Reedquist.** 2001. Rap1 signalling: adhering to new models. Nat. Rev. Mol. Cell Biol. 2:369–377.
7. **Chijiwa, T., A. Mishima, M. Hagiwara, M. Sano, K. Hayashi, T. Inoue, K. Naito, T. Toshioka, and H. Hidaka.** 1990. Inhibition of forskolin-induced neurite outgrowth and protein phosphorylation by a newly synthesized selective inhibitor of cyclic AMP-dependent protein kinase, N-[2-(p-bromocinnamylamino)ethyl]-5-isoquinolinesulfonamide (H-89), of PC12D pheochromocytoma cells. J. Biol. Chem. 265:5267–5272.
8. **Daly, R. J.** 2004. Cortactin signalling and dynamic actin networks. Biochem. J. 382:13–25. [Online.] doi:10.1042/BJ20040737.
9. **Dejana, E.** 2004. Endothelial cell-cell junctions: happy together. Nat. Rev. Mol. Cell Biol. 5:261–270.
10. **Dudek, S. M., and J. G. Garcia.** 2001. Cytoskeletal regulation of pulmonary vascular permeability. J. Appl. Physiol. 91:1487–1500.
11. **Dudek, S. M., J. R. Jacobson, E. T. Chiang, K. G. Birukov, P. Wang, X. Zhan, and J. G. Garcia.** 2004. Pulmonary endothelial cell barrier enhancement by sphingosine 1-phosphate: roles for cortactin and myosin light chain kinase. J. Biol. Chem. 279:24692–24700.
12. **Endo, A., K. Nagashima, H. Kurose, S. Mochizuki, M. Matsuda, and N. Mochizuki.** 2002. Sphingosine 1-phosphate induces membrane ruffling and increases motility of human umbilical vein endothelial cells via vascular endothelial growth factor receptor and CrkII. J. Biol. Chem. 277:23747–23754.
13. **Enserink, J. M., A. E. Christensen, J. de Rooij, M. van Triest, F. Schwede, H. G. Genieser, S. O. Doskeland, J. L. Blank, and J. L. Bos.** 2002. A novel Epac-specific cAMP analogue demonstrates independent regulation of Rap1 and ERK. Nat. Cell Biol. 4:901–906.
14. **Esser, S., M. G. Lampugnani, M. Corada, E. Dejana, and W. Risau.** 1998. Vascular endothelial growth factor induces VE-cadherin tyrosine phosphorylation in endothelial cells. J. Cell Sci. 111(Pt 13):1853–1865.
15. **Farmer, P. J., S. G. Bernier, A. Lepage, G. Guillemette, D. Regoli, and P. Sirois.** 2001. Permeability of endothelial monolayers to albumin is increased by bradykinin and inhibited by prostaglandins. Am. J. Physiol. Lung Cell. Mol. Physiol. 280:L732–L738.
16. **Fukuhara, S., M. J. Marinissen, M. Chiariello, and J. S. Gutkind.** 2000. Signaling from G protein-coupled receptors to ERK5/Big MAPK 1 involves Galpha q and Galpha 12/13 families of heterotrimeric G proteins. Evidence for the existence of a novel Ras AND Rho-independent pathway. J. Biol. Chem. 275:21730–21736.
17. **Gamble, J. R., J. Drew, L. Trezise, A. Underwood, M. Parsons, L. Kasminkas, J. Rudge, G. Yancopoulos, and M. A. Vadas.** 2000. Angiopoietin-1 is an antipermeability and anti-inflammatory agent in vitro and targets cell junctions. Circ. Res. 87:603–607.
18. **Garcia, J. G., F. Liu, A. D. Verin, A. Birukova, M. A. Dechert, W. T. Gerthoffer, J. R. Bamberg, and D. English.** 2001. Sphingosine 1-phosphate promotes endothelial cell barrier integrity by Edg-dependent cytoskeletal rearrangement. J. Clin. Investig. 108:689–701.
19. **Hippenstiel, S., M. Witzenrath, B. Schmeck, A. Hocke, M. Krisp, M. Krull, J. Seybold, W. Seeger, W. Rascher, H. Schutte, and N. Suttorp.** 2002. Adrenomedullin reduces endothelial hyperpermeability. Circ. Res. 91:618–625.
20. **Hogan, C., N. Serpente, P. Cogram, C. R. Hosking, C. U. Bialucha, S. M. Feller, V. M. M. Braga, W. Birchmeier, and Y. Fujita.** 2004. Rap1 regulates the formation of E-cadherin-based cell-cell contacts. Mol. Cell. Biol. 24:6690–6700.
21. **Kawasaki, H., G. M. Springett, N. Mochizuki, S. Toki, M. Nakaya, M. Matsuda, D. E. Housman, and A. M. Graybiel.** 1998. A family of cAMP-binding proteins that directly activate Rap1. Science 282:2275–2279.
22. **Kinbara, K., L. E. Goldfinger, M. Hansen, F. L. Chou, and M. H. Ginsberg.**

2003. Ras GTPases: integrins' friends or foes? Nat. Rev. Mol. Cell Biol. 4:767–776.
23. Knox, A. L., and N. H. Brown. 2002. Rap1 GTPase regulation of adherens junction positioning and cell adhesion. Science 295:1285–1288.
24. Kouklis, P., M. Konstantoulaki, S. Vogel, M. Broman, and A. B. Malik. 2004. Cdc42 regulates the restoration of endothelial barrier function. Circ. Res. 94:159–166.
25. Langeler, E. G., and V. W. van Hinsbergh. 1991. Norepinephrine and iloprost improve barrier function of human endothelial cell monolayers: role of cAMP. Am. J. Physiol. 260:C1052–C1059.
26. Lee, M. J., S. Thangada, K. P. Claffey, N. Ancellin, C. H. Liu, M. Kluk, M. Volpi, R. I. Sha'afi, and T. Hla. 1999. Vascular endothelial cell adherens junction assembly and morphogenesis induced by sphingosine-1-phosphate. Cell 99:301–312.
27. Lum, H., H. A. Jaffe, I. T. Schulz, A. Masood, A. RayChaudhury, and R. D. Green. 1999. Expression of PKA inhibitor (PKI) gene abolishes cAMP-mediated protection to endothelial barrier dysfunction. Am. J. Physiol. 277: C580–C588.
28. Maillet, M., S. J. Robert, M. Cacquevel, M. Gastineau, D. Vivien, J. Bertoglio, J. L. Zugaza, R. Fischmeister, and F. Lezoualc'h. 2003. Crosstalk between Rap1 and Rac regulates secretion of sAPPalpha. Nat. Cell Biol. 5:633–639.
29. Miles, A. A., and E. M. Miles. 1952. Vascular reactions to histamine, histamine-liberator and leukotaxine in the skin of guinea-pigs. J. Physiol. 118: 228–257.
30. Mochizuki, N., Y. Ohba, E. Kiyokawa, T. Kurata, T. Murakami, T. Ozaki, A. Kitabatake, K. Nagashima, and M. Matsuda. 1999. Activation of the ERK/MAPK pathway by an isoform of rap1GAP associated with G alpha(i). Nature 400:891–894.
31. Mori, Y., T. Nishikimi, N. Kobayashi, H. Ono, K. Kangawa, and H. Matsuoka. 2002. Long-term adrenomedullin infusion improves survival in malignant hypertensive rats. Hypertension 40:107–113.
32. Moy, A. B., J. E. Bodmer, K. Blackwell, S. Shasby, and D. M. Shasby. 1998. cAMP protects endothelial barrier function independent of inhibiting MLC20-dependent tension development. Am. J. Physiol. 274:L1024–L1029.
33. Navarro, P., L. Ruco, and E. Dejana. 1998. Differential localization of VE- and N-cadherins in human endothelial cells: VE-cadherin competes with N-cadherin for junctional localization. J. Cell Biol. 140:1475–1484.
34. Ohba, Y., K. Ikuta, A. Ogura, J. Matsuda, N. Mochizuki, K. Nagashima, K. Kurokawa, B. J. Mayer, K. Maki, J. Miyazaki, and M. Matsuda. 2001. Requirement for C3G-dependent Rap1 activation for cell adhesion and embryogenesis. EMBO J. 20:3333–3341.
35. Parandoosh, Z., C. A. Bogowitz, and M. P. Nova. 1998. A fluorometric assay for the measurement of endothelial cell density in vitro. In Vitro Cell. Dev. Biol. Anim. 34:772–776.
36. Price, L. S., A. Hajdo-Milasinovic, J. Zhao, F. J. Zwartkruis, J. G. Collard, and J. L. Bos. 2004. Rap1 regulates E-cadherin-mediated cell-cell adhesion. J. Biol. Chem. 279:35127–35132.
37. Quilliam, L. A., H. Mueller, B. P. Bohl, V. Prossnitz, L. A. Sklar, C. J. Der, and G. M. Bokoch. 1991. Rap1A is a substrate for cyclic AMP-dependent protein kinase in human neutrophils. J. Immunol. 147:1628–1635.
38. Shaywitz, A. J., and M. E. Greenberg. 1999. CREB: a stimulus-induced transcription factor activated by a diverse array of extracellular signals. Annu. Rev. Biochem. 68:821–861.
39. Stelzner, T. J., J. V. Weil, and R. F. O'Brien. 1989. Role of cyclic adenosine monophosphate in the induction of endothelial barrier properties. J. Cell. Physiol. 139:157–166.
40. Ukropec, J. A., M. K. Hollinger, S. M. Salva, and M. J. Woolkalis. 2000. SHP2 association with VE-cadherin complexes in human endothelial cells is regulated by thrombin. J. Biol. Chem. 275:5983–5986.
41. Yajnik, V., C. Paulding, R. Sordella, A. I. McClatchey, M. Saito, D. C. Wahrer, P. Reynolds, D. W. Bell, R. Lake, S. van den Heuvel, J. Settleman, and D. A. Haber. 2003. DOCK4, a GTPase activator, is disrupted during tumorigenesis. Cell 112:673–684.
42. Yano, H., Y. Mazaki, K. Kurokawa, S. K. Hanks, M. Matsuda, and H. Sabe. 2004. Roles played by a subset of integrin signaling molecules in cadherin-based cell-cell adhesion. J. Cell Biol. 166:283–295.
43. Yuan, S. Y. 2002. Protein kinase signaling in the modulation of microvascular permeability. Vascul. Pharmacol. 39:213–223.

Effects of Ghrelin Administration on Left Ventricular Function, Exercise Capacity, and Muscle Wasting in Patients With Chronic Heart Failure

Noritoshi Nagaya, MD; Junji Moriya, MD; Yoshio Yasumura, MD; Masaaki Uematsu, MD; Fumiaki Ono, MD; Wataru Shimizu, MD; Kazuyuki Ueno, PhD; Masafumi Kitakaze, MD; Kunio Miyatake, MD; Kenji Kangawa, PhD

Background—Ghrelin is a novel growth hormone–releasing peptide that also induces vasodilation, inhibits sympathetic nerve activity, and stimulates feeding through growth hormone–independent mechanisms. We investigated the effects of ghrelin on left ventricular (LV) function, exercise capacity, and muscle wasting in patients with chronic heart failure (CHF).

Methods and Results—Human synthetic ghrelin (2 μg/kg twice a day) was intravenously administered to 10 patients with CHF for 3 weeks. Echocardiography, cardiopulmonary exercise testing, dual x-ray absorptiometry, and blood sampling were performed before and after ghrelin therapy. A single administration of ghrelin elicited a marked increase in serum GH (25-fold). Three-week administration of ghrelin resulted in a significant decrease in plasma norepinephrine (1132±188 to 655±134 pg/mL; $P<0.001$). Ghrelin increased LV ejection fraction (27±2% to 31±2%; $P<0.05$) in association with an increase in LV mass and a decrease in LV end-systolic volume. Treatment with ghrelin increased peak workload and peak oxygen consumption during exercise. Ghrelin improved muscle wasting, as indicated by increases in muscle strength and lean body mass. These parameters remained unchanged in 8 patients with CHF who did not receive ghrelin therapy.

Conclusions—These preliminary results suggest that repeated administration of ghrelin improves LV function, exercise capacity, and muscle wasting in patients with CHF. (*Circulation.* **2004;110:3674-3679.**)

Key Words: growth substances ■ heart failure ■ hormones ■ nutrition

Left ventricular (LV) remodeling (dilatation and wall thinning) and cardiac cachexia (body weight loss and muscle wasting) often are observed in patients with end-stage chronic heart failure (CHF).[1,2] Growth hormone (GH) and its mediator, insulinlike growth factor-1 (IGF-1), are anabolic hormones that are essential for skeletal and myocardial growth and metabolic homeostasis.[3,4] Earlier studies have shown that GH supplementation may have beneficial effects on LV myocardial structure and function in some patients with CHF,[5] although the importance of GH resistance[6] and neutral results of randomized trials also have been reported.[7,8]

Ghrelin is a novel GH-releasing peptide that was isolated from the stomach and has been identified as an endogenous ligand for the growth hormone secretagogue receptor.[9] Therefore, we believed that administration of ghrelin may induce beneficial changes in LV function and energy metabolism in patients with CHF via a GH-dependent mechanism. On the other hand, growth hormone secretagogue receptor mRNA is detected not only in the hypothalamus and pituitary but also in the heart and blood vessels,[10] implying direct cardiovascular effects of ghrelin. Wiley and Davenport[11] have demonstrated that ghrelin is an endothelium-independent vasodilator in isolated human arteries. We have shown that intravenous administration of ghrelin decreases systemic vascular resistance and increases cardiac output in patients with CHF.[12] Furthermore, ghrelin induces a positive energy balance by stimulating food intake[13,14] and adiposity[15] through GH-independent mechanisms. These findings raise the possibility that ghrelin administration may have beneficial effects in cachectic patients with CHF. In fact, we recently have demonstrated that treatment with ghrelin improves not only LV function but also cardiac cachexia in rats with CHF.[16] In humans, however, the potential effects of ghrelin as a therapeutic agent for CHF remain unknown.

Thus, the purposes of this study were as follows: (1) to investigate whether repeated administration of ghrelin im-

Received April 30, 2004; revision received July 6, 2004; accepted August 23, 2004.

From the Department of Internal Medicine, National Cardiovascular Center, Osaka (N.N., J.M., Y.Y., F.O., W.S., M.K., K.M.); Cardiovascular Division, Kansai Rosai Hospital, Hyogo (M.U.); and Departments of Pharmacy (K.U.) and Biochemistry (K.K.), National Cardiovascular Center Research Institute, Osaka, Japan.

Reprint requests to Noritoshi Nagaya, MD, Department of Internal Medicine, National Cardiovascular Center, 5-7-1 Fujishirodai, Suita, Osaka 565-8565, Japan. E-mail nagayann@hsp.ncvc.go.jp

© 2004 American Heart Association, Inc.

Circulation is available at http://www.circulationaha.org

DOI: 10.1161/01.CIR.0000149746.62908.BB

TABLE 1. Patient Characteristics

	Control Group (n=8)	Ghrelin Group (n=10)
Age, y	74±2	75±2
Sex, M/F	6/2	7/3
Body mass index, kg/m²	19.0±1.1	19.0±0.9
Cause of CHF, n		
Dilated cardiomyopathy	4	4
Ischemic cardiomyopathy	1	3
Hypertensive heart disease	2	1
Valvular heart disease	1	2
NYHA functional class, n		
III	8	9
IV	0	1
LVEF, %	28±2	27±2
Presence of cardiac cachexia, n	6	8
Medication use, n		
Digoxin	6	9
ACE inhibitors	7	9
A II blockers	2	2
β-Blockers	6	7
Diuretics	7	10

LVEF indicates LV ejection fraction; A II, angiotensin II. Data are mean±SEM.

proves LV myocardial structure and function in patients with CHF, (2) to examine whether ghrelin improves exercise capacity in such patients, and (3) to examine whether ghrelin induces anabolic effects in patients with CHF.

Methods

Study Subjects

Eighteen patients with CHF (13 men, 5 women; mean age, 75 years; range, 63 to 80 years) were included in this study. Inclusion criteria were as follows: (1) LV ejection fraction <35% as assessed by cardiac catheterization, (2) a stable clinical condition, and (3) clinical evidence of heart failure despite conventional therapy. Exclusion criteria were the presence of any of the following: (1) chronic renal impairment (serum creatinine level ≥2.0 mg/dL), (2) significant liver dysfunction, (3) evidence of malignant diseases, (4) active infection, (5) hematologic abnormalities, or (6) systolic blood pressure <90 mm Hg. Ten patients with CHF (ghrelin group) received repeated administrations of ghrelin. Although this study was neither randomized nor placebo controlled, 8 patients with CHF who did not receive ghrelin (control group) were studied to exclude time-course effects during hospitalization. Patients in the ghrelin group were admitted only for the study. Those in the control group had been in hospital for diagnostic examination and stayed for 3 weeks for the study. There was no significant difference in demographic, clinical, or hemodynamic data at baseline between the ghrelin and control groups (Table 1). Eight patients in the ghrelin group and 6 patients in the control group were defined as exhibiting cardiac cachexia, as reported previously.[17] The weight loss in cachectic patients amounted to 6.4±0.4 kg or 11.8±0.7% loss of previous body weight during 14±2 months. The ethics committee of the National Cardiovascular Center approved the study, and all patients gave written informed consent.

Preparation of Human Ghrelin

Human synthetic ghrelin was obtained from the Peptide Institute Inc. This peptide is not commercially available. Ghrelin was dissolved in distilled water with 4% D-mannitol and sterilized by passage through a 0.22-μm filter (Millipore Co). Ghrelin was stored in 2-mL volumes, each containing 200 μg ghrelin. The chemical nature and content of the human ghrelin in vials were verified by high-performance liquid chromatography and radioimmunoassay. All vials were stored frozen at −80°C from the time of dispensing until the time of preparation for administration.

Study Protocol

This study was performed while patients were in a stable clinical condition during hospitalization. Ghrelin (2 μg/kg, 10 mL solution) was administered intravenously over 30 minutes at a constant rate. The infusion was repeated twice a day (before breakfast and before dinner) for 3 weeks. Study patients in both groups remained hospitalized for 3 weeks. Echocardiography, cardiopulmonary exercise testing, dual x-ray absorptiometry, hand-grip test, and blood sampling were performed at baseline and after 3 weeks of treatment with ghrelin (ghrelin group) or without ghrelin (control group). Long-term medication, including digitalis, diuretics, ACE inhibitors, and β-blockers, was kept constant during this study protocol.

Echocardiographic Studies

Echocardiography was performed by an investigator blinded to treatment allocation. Two-dimensional targeted M-mode tracings were obtained at the level of the papillary muscles with an echocardiographic system equipped with a 3.5-MHz sector scan probe (SONOS 2000, Hewlett Packard). LV wall thickness, dimensions, and fractional shortening were measured according to the recommendations of the American Society of Echocardiology from at least 3 consecutive cardiac cycles. LV end-diastolic volume, end-systolic volume, and ejection fraction were calculated with a modified version of Simpson's method.[18]

Cardiopulmonary Exercise Testing

Cardiopulmonary exercise testing was performed in all patients except 1, who underwent a 6-minute walk test as recommended by attending physicians. The patients exercised seated on a cycle ergometer. The work rate was then increased by 15 W/min up to their symptom-limited maximum. Breath-by-breath gas analysis was performed with an AE280 (Minato Medical Science).[19] Exercise capacity was evaluated by peak oxygen consumption (peak $\dot{V}O$). Ventilatory efficiency during exercise was represented by the $\dot{V}E$–$\dot{V}CO_2$ slope.[19]

Food Intake and Body Mass Analyses

Food intake for 3 consecutive days was assessed before ghrelin administration and during the last week of ghrelin therapy. Food intake was semiquantitatively assessed by a calorie count based on a 10-point scale method (0=null intake, 10=full intake or 1800 kcal), which was averaged for 3 days. Dual x-ray absorptiometry (DPX-L, Lunar Radiation) was repeated in all patients to examine changes in lean body mass, fat mass, and bone mineral content. Hand-grip strength was determined with a dynamometer.

Blood Sampling and Assay

Blood samples were taken from the antecubital vein the morning after an overnight fast. Serum GH and IGF-1 were measured by immunoradiometric assay (Ab Bead HGH Eiken, Eiken Chemical Co, Ltd, sensitivity=0.1 ng/mL; Somatomedin CII Bayer, Bayer Medical Ltd, sensitivity=0.3 ng/mL). Plasma norepinephrine and epinephrine were measured by high-performance liquid chromatography (HLC8030, Tosoh Co, sensitivity=6 pg/mL). Serum cortisol and insulin were measured by enzyme immunoassay (AIA-PACK CORT, sensitivity=0.2 μg/dL; AIA-PACK IRI, sensitivity=2.0 μU/mL, Tosoh Co). Serum tumor necrosis factor (TNF-α) and interleukin-6 (IL-6) were measured by enzyme immunoassay (Quantikine HS, R&D Systems Inc, sensitivity=0.18 pg/mL; TFB kit, TFB Co, Ltd, sensitivity=0.3 pg/mL). Plasma renin and aldosterone were measured with radioimmunoassay kits (RENIN RIABEAD, sensitivity=0.1 ng/mL; ALDOSTERONE RIAKIT II, sensitivity=2.0

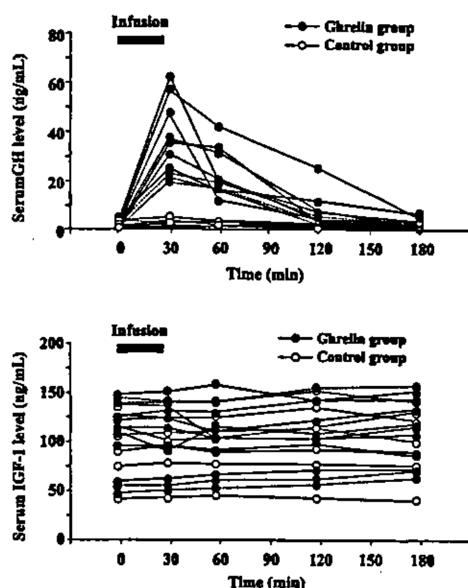

Figure 1. Changes in serum GH and IGF-1 after single administration of ghrelin. Solid line indicates cachectic patients; dotted line, noncachectic patients.

ng/dL, DAINABOT Co). Plasma brain natriuretic peptide (BNP) was measured by immunoradiometric assay (SHIONORIA BNP, sensitivity=4.0 pg/mL).

Statistical Analysis

Numerical values are expressed as mean±SEM. Comparisons of parameters between the 2 groups were made by unpaired Student's *t* test. Comparisons of the time course of serum GH and IGF-1 between the 2 groups were made by 2-way ANOVA for repeated measures, followed by the Newman-Keuls test. Comparisons of changes in parameters during the 3-week follow-up between the 2 groups were also made by 2-way ANOVA for repeated measures, followed by the Newman-Keuls test. A value of $P<0.05$ was considered significant.

Results

Administration of ghrelin transiently caused stomach rumbles in 6 patients and a slight feeling of being warm and sleepy in 4 subjects. Two patients felt slightly thirsty during ghrelin infusion. Other than these minor complaints, all subjects tolerated 3-week administration of ghrelin without incident. After 3-week administration of ghrelin, NYHA functional class improved in 4 patients and was unchanged in 6 patients. No change in NYHA functional class was observed in patients who did not receive ghrelin.

Effects of Ghrelin on Somatotropic Function

A single administration of ghrelin markedly increased serum GH level (baseline, 1.4±0.4; peak, 35.0±5.0 ng/mL; $P<0.001$; Figure 1). This elevation lasted >60 minutes after the start of ghrelin infusion. Serum IGF-1 level tended to increase 3 hours after the start of ghrelin infusion (101±12 to 110±12 ng/mL; $P=0.08$). Three-week administration of ghrelin tended to increase basal serum IGF-1 level (99±13 to 116±13 ng/mL; $P=0.07$). There was no significant difference in basal serum GH level between before and after 3 weeks of ghrelin therapy (2.0±0.8 to 1.2±0.3 ng/mL; $P=$NS).

Effects of Ghrelin on Food Intake, Body Weight, and Lean Body Mass

Administration of ghrelin significantly increased food intake (Figure 2). Three-week administration of ghrelin tended to increase body weight (49.6±2.7 to 50.4±2.7 kg; $P=0.09$). No development of edema was observed during ghrelin therapy. Dual x-ray absorptiometry demonstrated that treatment with ghrelin significantly increased lean body mass in patients with CHF (38.3±2.1 to 39.1±2.1 kg; $P<0.05$). Ghrelin did not significantly alter bone mineral content (2243±191 to 2265±189 g; $P=$NS) or fat mass (8877±1353 to 8748±1311 g; $P=$NS). Hand-grip strength was increased significantly by ghrelin therapy (20.5±1.7 to 22.7±2.0 kg; $P<0.01$). All of these parameters remained unchanged in patients who did not receive ghrelin.

Effects of Ghrelin on Cardiac Structure and Function

Neither heart rate nor blood pressure was significantly changed by 3-week administration of ghrelin (Table 2). Ghrelin increased LV ejection fraction (27±2% to 31±2%; $P<0.05$) in association with a decrease in LV end-systolic volume and an increase in LV mass (Figure 3), although ghrelin did not significantly alter LV end-diastolic volume. All of these parameters remained unchanged in patients who did not receive ghrelin.

Effects of Ghrelin on Exercise Capacity and Ventilatory Efficiency

Three-week administration of ghrelin significantly increased peak workload and peak $\dot{V}O$ during exercise (739±127 to 801±126 mL/min; $P<0.05$; Figure 4). Treatment with ghrelin did not significantly alter the $\dot{V}E$–$\dot{V}CO_2$ slope. In 1 patient

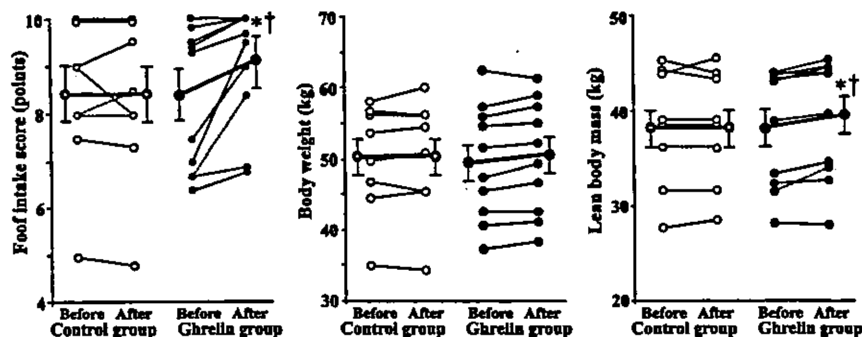

Figure 2. Food intake, body weight, and lean body mass before and after 3-week administration of ghrelin. Food intake was described semiquantitatively with 10-point scale method (0=null intake, 10=full intake). Data are mean±SEM. Solid line indicates cachectic patients; dotted line, noncachectic patients. *$P<0.05$ vs before; †$P<0.05$ vs respective control group.

TABLE 2. Physiological and Echocardiographic Measurements

	Control Group	Ghrelin Group
Heart rate, bpm		
Before	77±3	78±3
After	76±3	74±3
Mean arterial pressure, mm Hg		
Before	79±4	81±2
After	80±3	78±3
LVDd, mm		
Before	65.6±3.2	66.6±2.5
After	64.4±3.7	63.7±3.3
LVDs, mm		
Before	55.1±3.0	56.9 ± 2.9
After	53.9±3.6	52.8 ± 3.4*
FS, %		
Before	16.1±1.2	14.8±1.7
After	16.0±1.3	17.3±2.3
AWT diastole, mm		
Before	10.0±0.8	9.5±1.0
After	10.1±0.9	10.0±1.0*
PWT diastole, mm		
Before	9.2±0.4	9.3±0.6
After	9.4±0.4	9.9±0.5*†

LVDd indicates LV end-diastolic dimension; LVDs, LV end-systolic dimension; FS, fractional shortening; AWT, anterior wall thickness; and PWT, posterior wall thickness. Data are mean±SEM.

*$P<0.05$ vs before; †$P<0.05$ vs respective control group.

who did not undergo cardiopulmonary exercise testing, the distance walked in 6 minutes increased from 300 m to 410 m with ghrelin treatment. Exercise parameters remained unchanged without ghrelin.

Effects of Ghrelin on Sympathetic Nerve Activity

Three-week administration of ghrelin significantly decreased plasma norepinephrine and epinephrine (Figure 5). Treatment with ghrelin significantly decreased plasma BNP level (Table 3). Ghrelin did not significantly alter circulating glucose, insulin, cortisol, TNF-α, or IL-6. Neither plasma renin activity nor plasma aldosterone level was changed significantly. All of these parameters remained unchanged in patients who did not receive ghrelin.

Discussion

Ghrelin is a novel GH-releasing peptide that acts through a mechanism independent of that of hypothalamic GH-releasing hormone.[9] The GH-releasing effect of ghrelin has been shown to be more potent than that of GH-releasing hormone.[20] In fact, in the present study, ghrelin infusion elicited potent GH release in patients with CHF. Three-week administration of ghrelin increased LV ejection fraction in association with an increase in LV mass, which is consistent with findings from a previous experimental study in rats.[16] Plasma BNP level, a marker for LV function and wall stress, was decreased by ghrelin therapy. GH and its mediator, IGF-1, have been shown to enhance physiological compensatory hypertrophy in rats with CHF, resulting in a decrease in LV wall stress, leading to improvement in cardiac function.[21] Thus, ghrelin may also improve cardiac function partly through GH-dependent mechanisms. On the other hand, Baldanzi et al[22] have shown that ghrelin inhibits apoptosis of cardiomyocytes and endothelial cells through activation of extracellular signal-regulated kinase-1/2 and Akt serine kinases. Furthermore, stimulation of GHS-R by hexarelin has been shown to prevent cardiac damage after ischemia-reperfusion in hypophysectomized rats.[23] When these results are considered together, improvement in cardiac function by ghrelin therapy may be related to direct effects of ghrelin on myocardium. Importantly, ghrelin significantly decreased plasma norepinephrine levels in the present study. It is possible that improvement in cardiac function may lead to attenuation of sympathetic nerve activity. Interestingly, a recent study has demonstrated that ghrelin acts directly on the central nerve system to decrease sympathetic nerve activity.[24] Thus, inhibitory effects of ghrelin on sympathetic nerve activity may contribute to a decrease in plasma norepinephrine, which may have beneficial effects on cardiac performance in patients with CHF.

In the present study, 3-week administration of ghrelin improved exercise capacity in patients with CHF, as indicated by an increase in peak workload and peak V̇o. A decrease in peak V̇o in patients with CHF is attributable not only to an inadequate increase in cardiac output during exercise, which is a central effect, but also to muscle wasting, a peripheral effect. Recently, we have shown that infusion of ghrelin increases cardiac output in patients with CHF.[12] In the present study, ghrelin increased lean body mass and muscle strength. These results suggest that ghrelin may improve exercise capacity through both central and peripheral effects.

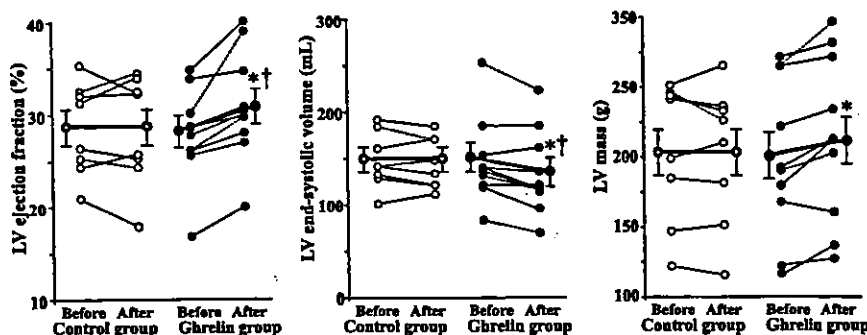

Figure 3. LV geometry and function before and after ghrelin therapy. Data are mean±SEM. Solid line indicates cachectic patients; dotted line, noncachectic patients. *$P<0.05$ vs before; †$P<0.05$ vs respective control group.

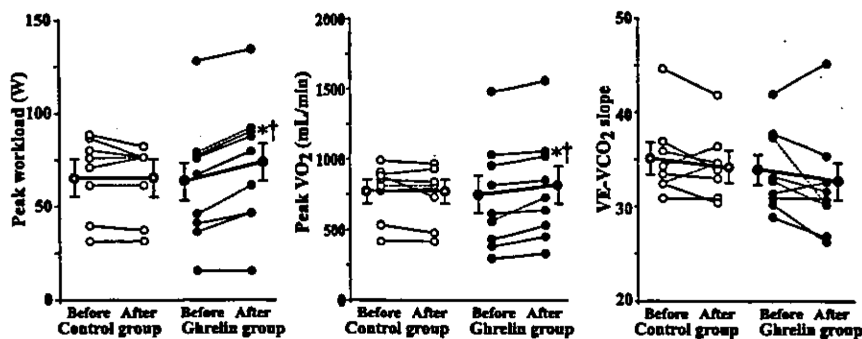

Figure 4. Exercise capacity and ventilatory efficiency before and after ghrelin therapy. Data are mean±SEM. Solid line indicates cachectic patients; dotted line, noncachectic patients. *$P<0.05$ vs before; †$P<0.05$ vs respective control group.

Cardiac cachexia, a catabolic state characterized by weight loss and muscle wasting, occurs frequently in patients with end-stage CHF[25] and is a strong independent risk factor for mortality in such patients.[26] Recently, we have shown that plasma ghrelin level is increased in cachectic patients with CHF as a compensatory mechanism in response to anabolic-catabolic imbalance.[17] In the present study, 3-week administration of ghrelin tended to increase body weight and significantly increased lean body mass and muscle strength. These results suggest that treatment with ghrelin improves muscle wasting in patients with CHF. These effects may be mediated, at least in part, by GH/IGF-1, which is considered essential for skeletal muscle. Earlier studies have shown that ghrelin induces orexigenic effects via activation of neuropeptide Y neurons in the hypothalamic arcuate nucleus.[13,14] In the present study, intravenous administration of ghrelin increased food intake in patients with CHF, which may contribute to anabolic effects of ghrelin. Tschop et al[15] have shown that administration of ghrelin induces adiposity through a GH-independent mechanism. In the present study, however, ghrelin did not significantly increase fat mass. This difference may be explained by the high dose of ghrelin (>2000-fold) used by Tschop et al. Ghrelin itself decreases fat utilization and increases fat, whereas GH decreases fat tissue and increases lean tissue. Thus, in the present study, ghrelin-induced GH may have attenuated an increase in fat and enhanced an increase in lean tissue.

The major limitation of this pilot trial relates to the lack of a randomized, placebo-controlled group. Patients in the control group were not treated identically because a placebo infusion was not performed. Nonetheless, this study was performed while patients were in a stable clinical condition during hospitalization. In addition, 8 patients in the control group were studied to exclude time-course effects during hospitalization. On the basis of the results of this study, a double-blind, randomized, and placebo-controlled study should be conducted. Second, this clinical study did not clarify mechanisms of increased LV ejection fraction by ghrelin therapy. Further studies are necessary to examine which mechanism predominantly contributes to improvement in LV ejection fraction.

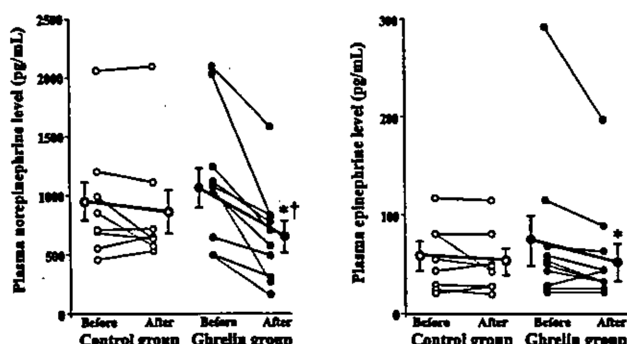

Figure 5. Plasma levels of norepinephrine and epinephrine before and after ghrelin therapy. Data are mean±SEM. Solid line indicates cachectic patients; dotted line, noncachectic patients. *$P<0.05$ vs before; †$P<0.05$ vs respective control group.

Except for a few minor complications, long-term treatment with ghrelin was tolerated well in patients with CHF. Although a preliminary study documented the beneficial effects

TABLE 3. Hormone Analysis in Patients With CHF

	Control Group	Ghrelin Group
BNP, pg/mL		
Before	180±53	238±59
After	181±62	190±60*
Fasting glucose, mg/dL		
Before	105±5	101±4
After	102±6	102±7
Insulin, μU/mL		
Before	6.0±1.4	3.9±0.7
After	6.8±2.0	5.5±1.2
Cortisol, μg/dL		
Before	15.5±1.9	17.9±1.6
After	14.5±2.6	17.2±1.5
TNF-α, pg/mL		
Before	5.3±0.9	5.7±0.8
After	5.4±0.9	5.6±0.8
IL-6, pg/mL		
Before	3.2±0.5	3.8±0.7
After	3.4±0.5	3.6±0.7
Renin, ng · mL^{-1} · h^{-1}		
Before	9.3±4.6	7.3±3.0
After	10.1±4.1	6.9±3.7
Aldosterone, ng/dL		
Before	11.6±4.1	15.0±4.7
After	12.7±4.1	11.9±4.2

Data are mean±SEM.
*$P<0.05$ vs before.

of GH,[5] controlled studies in humans have been predominantly negative.[7,8] Nevertheless, ghrelin has been shown to have GH-independent effects, stimulating vasodilation,[10-12] reversing cachexia,[13-15] and inhibiting sympathetic nerve activity[24] and myocyte apoptosis.[22] Thus, ghrelin may have additional therapeutic potential compared with GH supplementation. Ghrelin improved cardiac function and exercise capacity in not only cachectic CHF patients but also noncachectic ones. Nevertheless, the best candidates may be cachectic CHF patients because ghrelin stimulates feeding and improves muscle wasting.

Conclusions

These preliminary results suggest that repeated administration of ghrelin improves LV structure and function, exercise capacity, and muscle wasting in patients with CHF. Thus, administration of ghrelin may be a new therapeutic approach for the treatment of CHF.

Acknowledgments

This work was supported by Research Grant for Cardiovascular Disease 16C-6 from the Ministry of Health, Labor and Welfare; Industrial Technology Research Grant Program in 2003 from the New Energy and Industrial Technology Development Organization of Japan; Health and Labor Sciences Research Grants–Genome 005, Mochida Memorial Foundation for Medical and Pharmaceutical Research; and the Promotion of Fundamental Studies in Health Science of the Organization for Pharmaceutical Safety and Research of Japan.

References

1. Dec GW, Fuster V. Idiopathic dilated cardiomyopathy. *N Engl J Med.* 1994;331:1564–1575.
2. Pittman JG, Cohen P. The pathogenesis of cardiac cachexia. *N Engl J Med.* 1964;271:403–409.
3. Amato G, Carella C, Fazio S, et al. Body composition, bone metabolism, heart structure and function in growth hormone deficient adults before and after growth hormone replacement therapy at low doses. *J Clin Endocrinol Metab.* 1993;77:1671–1676.
4. Fuller J, Mynett JR, Sugden PH. Stimulation of cardiac protein synthesis by insulin-like growth factors. *Biochem J.* 1992;282:85–90.
5. Fazio S, Sabatini D, Capaldo B, et al. A preliminary study of growth hormone in the treatment of dilated cardiomyopathy. *N Engl J Med.* 1996;334:809–814.
6. Anker SD, Volterrani M, Pflaum CD, et al. Acquired growth hormone resistance in patients with chronic heart failure: implications for therapy with growth hormone. *J Am Coll Cardiol.* 2001;38:443–452.
7. Osterziel KJ, Strohm O, Schuler J, et al. Randomised, double-blind, placebo-controlled trial of human recombinant growth hormone in patients with chronic heart failure due to dilated cardiomyopathy. *Lancet.* 1998;351:1233–1237.
8. Isgaard J, Bergh CH, Caidahl K, et al. A placebo-controlled study of growth hormone in patients with congestive heart failure. *Eur Heart J.* 1998;19:1704–1711.
9. Kojima M, Hosoda H, Date Y, et al. Ghrelin is a growth-hormone–releasing acylated peptide from stomach. *Nature.* 1999;402: 656–660.
10. Nagaya N, Kojima M, Uematsu M, et al. Hemodynamic and hormonal effects of human ghrelin in healthy volunteers. *Am J Physiol Regul Integr Comp Physiol.* 2001;280:R1483–R1487.
11. Wiley KE, Davenport AP. Comparison of vasodilators in human internal mammary artery: ghrelin is a potent physiological antagonist of endothelin-1. *Br J Pharmacol.* 2002;136:1146–1152.
12. Nagaya N, Miyatake K, Uematsu M, et al. Hemodynamic, renal and hormonal effects of ghrelin infusion in patients with chronic heart failure. *J Clin Endocrinol Metab.* 2001;86:5854–5859.
13. Nakazato M, Murakami N, Date Y, et al. A role for ghrelin in the central regulation of feeding. *Nature.* 2001;409:194–198.
14. Shintani M, Ogawa Y, Ebihara K, et al. Ghrelin, an endogenous growth hormone secretagogue, is a novel orexigenic peptide that antagonizes leptin action through the activation of hypothalamic neuropeptide Y/Y1 receptor pathway. *Diabetes.* 2001;50:227–232.
15. Tschop M, Smiley DL, Heiman ML. Ghrelin induces adiposity in rodents. *Nature.* 2000;407:908–913.
16. Nagaya N, Uematsu M, Kojima M, et al. Chronic administration of ghrelin improves left ventricular dysfunction and attenuates development of cardiac cachexia in rats with heart failure. *Circulation.* 2001;104: 1430–1435.
17. Nagaya N, Uematsu M, Kojima M, et al. Elevated circulating levels of ghrelin in the cachexia associated with chronic heart failure. *Circulation.* 2001;104:2034–2038.
18. Schiller NB, Acquatella H, Ports TA, et al. Left ventricular volume from paired biplane two-dimensional echocardiography. *Circulation.* 1979;60: 547–555.
19. Nagaya N, Uematsu M, Oya H, et al. Short-term oral administration of L-arginine improves hemodynamics and exercise capacity in patients with precapillary pulmonary hypertension. *Am J Respir Crit Care Med.* 2001; 163:887–891.
20. Takaya K, Ariyasu H, Kanamoto N, et al. Ghrelin strongly stimulates growth hormone (GH) release in humans. *J Clin Endocrinol Metab.* 2000;85:4908–4911.
21. Cittadini A, Grossman JD, Napoli R, et al. Growth hormone attenuates early left ventricular remodeling and improves cardiac function in rats with large myocardial infarction. *J Am Coll Cardiol.* 1997;29: 1109–1116.
22. Baldanzi G, Filigheddu N, Cutrupi S, et al. Ghrelin and des-acyl ghrelin inhibit cell death in cardiomyocytes and endothelial cells through ERK1/2 and PI 3-kinase/AKT. *J Cell Biol.* 2002;159:1029–1037.
23. Locatelli V, Rossoni G, Schweiger F, et al. Growth hormone–independent cardioprotective effects of hexarelin in the rat. *Endocrinology.* 1999;140: 4024–4031.
24. Matsumura K, Tsuchihashi T, Fujii K, et al. Central ghrelin modulates sympathetic activity in conscious rabbits. *Hypertension.* 2002;40: 694–699.
25. Anker SD, Negassa A, Coats AJ, et al. Prognostic importance of weight loss in chronic heart failure and the effect of treatment with angiotensin-converting-enzyme inhibitors: an observational study. *Lancet.* 2003;361: 1077–1083.
26. Anker SD, Ponikowski P, Varney S, et al. Wasting as independent risk factor for mortality in chronic heart failure. *Lancet.* 1997;349: 1050–1053.

Adrenomedullin Enhances Angiogenic Potency of Bone Marrow Transplantation in a Rat Model of Hindlimb Ischemia

Takashi Iwase, MD; Noritoshi Nagaya, MD; Takafumi Fujii, MD; Takefumi Itoh, MD; Hatsue Ishibashi-Ueda, MD; Masakazu Yamagishi, MD; Kunio Miyatake, MD; Toshio Matsumoto, MD; Soichiro Kitamura, MD; Kenji Kangawa, PhD

Background—Previous studies have shown that adrenomedullin (AM) inhibits vascular endothelial cell apoptosis and induces angiogenesis. We investigated whether AM enhances bone marrow cell–induced angiogenesis.

Methods and Results—Immediately after hindlimb ischemia was created, rats were randomized to receive AM infusion plus bone marrow–derived mononuclear cell (MNC) transplantation (AM+MNC group), AM infusion alone (AM group), MNC transplantation alone (MNC group), or vehicle infusion (control group). The laser Doppler perfusion index was significantly higher in the AM and MNC groups than in the control group (0.74±0.11 and 0.69±0.07 versus 0.59±0.07, respectively, $P<0.01$), which suggests the angiogenic potency of AM and MNC. Importantly, improvement in blood perfusion was marked in the AM+MNC group (0.84±0.08). Capillary density was highest in the AM+MNC group, followed by the AM and MNC groups. In vitro, AM inhibited MNC apoptosis, promoted MNC adhesiveness to a human umbilical vein endothelial cell monolayer, and increased the number of MNC-derived endothelial progenitor cells. In vivo, AM administration not only enhanced the differentiation of MNC into endothelial cells but also produced mature vessels that included smooth muscle cells.

Conclusions—A combination of AM infusion and MNC transplantation caused significantly greater improvement in hindlimb ischemia than MNC transplantation alone. This effect may be mediated in part by the angiogenic potency of AM itself and the beneficial effects of AM on the survival, adhesion, and differentiation of transplanted MNCs. ***(Circulation*. 2005;111:356-362.)**

Key Words: peptides ■ angiogenesis ■ peripheral vascular disease

Peripheral vascular disease is a crucial health issue that affects an estimated 27 million people.[1] Despite recent advances in medical intervention, the symptoms of some patients with critical limb ischemia fail to be controlled. Bone marrow–derived mononuclear cells (MNCs) include a variety of stem and progenitor cells, such as endothelial progenitor cells (EPCs), and contribute to pathological neovascularization.[2] MNC transplantation induces therapeutic angiogenesis in ischemic limb[3,4]; however, some patients fail to respond to this cell therapy. Thus, a novel therapeutic strategy to enhance the angiogenic property of MNCs is desirable.

Adrenomedullin (AM) is a potent vasodilator peptide that was originally isolated from human pheochromocytoma.[5] Previous studies have reported that abnormalities of vascular structure are present in homozygous AM knockout mice.[6,7] A recent study has demonstrated that blood flow recovery in ischemic limb and tumor angiogenesis are substantially impaired in heterozygous AM knockout mice.[8] Furthermore, AM has been shown to inhibit vascular endothelial cell apoptosis and induce angiogenesis through the activation of the phosphatidylinositol 3-kinase (PI3K)/Akt pathway.[9,10] These results suggest that AM is indispensable for modulating angiogenesis and vasculogenesis. When these findings are taken together, combination therapy with MNC transplantation and AM infusion may have additional or synergetic effects on therapeutic angiogenesis for the treatment of severe peripheral vascular disease. Thus, the purposes of the present study were (1) to investigate whether local infusion of AM enhances the angiogenic potency of MNC transplantation in a rat model of hindlimb ischemia and (2) to investigate the effects of AM on the survival, adhesion, and differentiation of transplanted MNCs.

Received June 18, 2004; revision received September 9, 2004; accepted November 3, 2004.

From the Departments of Regenerative Medicine and Tissue Engineering (T. Iwase, N.N., T. Itoh), Cardiac Physiology (T.F.), and Biochemistry (K.K.), National Cardiovascular Center Research Institute, Osaka, Japan; Departments of Internal Medicine (N.N., M.Y., K.M.), Pathology (H.I.-U.), and Cardiovascular Surgery (S.K.), National Cardiovascular Center, Osaka, Japan; and Department of Medicine and Bioregulatory Sciences (T. Iwase, T.M.), University of Tokushima Graduate School of Medicine, Tokushima, Japan.

Reprint requests to Noritoshi Nagaya, MD, Department of Regenerative Medicine and Tissue Engineering, National Cardiovascular Center Research Institute, 5-7-1 Fujishirodai, Suita, Osaka 565-8565, Japan. E-mail nagayann@hsp.ncvc.go.jp

© 2005 American Heart Association, Inc.

Circulation is available at http://www.circulationaha.org

DOI: 10.1161/01.CIR.0000153352.29335.B9

Methods

Animal Model of Hindlimb Ischemia

Male Lewis rats (weight 250 to 275 g; Japan SLC Inc, Hamamatsu, Japan) were used in the present study. The left common iliac artery of each rat was resected under anesthesia with pentobarbital sodium (50 mg/kg). The distal portion of the saphenous artery and all side branches and veins were dissected free and excised. The right hindlimb was kept intact and used as the nonischemic limb. Transplantation of bone marrow–derived MNCs and infusion of AM were performed in 40 rats immediately after hindlimb ischemia was created. This protocol resulted in the creation of 4 groups: (1) AM infusion plus MNC transplantation (AM+MNC group, n=10), (2) AM infusion plus PBS injection (AM group, n=10), (3) vehicle infusion plus MNC transplantation (MNC group, n=10), and (4) vehicle infusion plus PBS injection (control group, n=10). The Animal Care Committee of the National Cardiovascular Center approved this experimental protocol.

MNC Transplantation and AM Infusion

Bone marrow was harvested from the femur and tibia in other male Lewis rats, and MNCs were isolated by Ficoll density gradient centrifugation (Lymphoprep, Nycomed). MNCs (5×10^6 cells per animal) or PBS was injected into the ischemic thigh muscle with a 26-gauge needle at 5 different points. Human recombinant AM (0.01 $\mu g \cdot kg^{-1} \cdot min^{-1}$) or vehicle was administered for 7 days with a mini-osmotic pump (ALZET, Palo Alto) implanted in the left inguinal region.

Assessment of Blood Perfusion

To measure serial blood flow for 3 weeks, we used a laser Doppler perfusion image (LDPI) analyzer (Moor Instrument). After blood flow was scanned twice, the average flow values of the ischemic and nonischemic limbs were calculated by computer-assisted quantification. The LDPI index was determined as the ratio of ischemic to nonischemic hindlimb blood perfusion.[11]

Histological Assessment

Three weeks after MNC transplantation and/or AM infusion, 4 pieces of ischemic tissue from the adductor and semimembranous muscles were obtained and snap-frozen in liquid nitrogen. Frozen tissue sections were stained with alkaline phosphatase by an indoxyl tetrazolium method to detect capillary endothelial cells.[3,11] Five fields were randomly selected to count the number of capillaries. The capillary number adjusted per muscle fiber was used to compare the differences in capillary density among the 4 groups.[3]

Monitoring of Transplanted MNCs in Ischemic Hindlimb Muscle

To examine differentiation of transplanted MNCs, 5×10^6 MNCs labeled with red fluorescent dye (PKH26-GL, Sigma Chemical Co) were transplanted into the ischemic thigh muscle in rats with (n=3) and without (n=3) AM infusion. Three weeks after transplantation, frozen tissue sections from ischemic muscle were incubated with anti-von Willebrand factor antibody (vWF, DAKO), anti-CD31 antibody (BD Pharmingen), and anti-α-smooth muscle actin antibody (α-SMA, DAKO), followed by incubation with Alexa Fluor 633 IgG antibody (Molecular Probes) and FITC-conjugated IgG antibody (BD Pharmingen), respectively. Five high-power fields (40×) of each section were randomly selected to count the number of transplanted MNCs, vWF-positive cells, and α-SMA–positive cells.

In Situ Detection of MNC Apoptosis

PKH26-labeled MNCs (5×10^6 cells per animal) were transplanted into the ischemic muscle in rats with (n=2) and without (n=2) AM infusion. Twenty-four hours after transplantation, apoptosis of transplanted MNCs in ischemic tissue was evaluated by terminal dUTP nick-end labeling (TUNEL) assay (ApopTag Fluorescein kit, Serological Corporation), as reported previously.[12]

In Vitro Apoptosis Assay

The antiapoptotic effect of AM on MNCs was evaluated by TUNEL assay. Human MNCs, isolated from peripheral blood, were plated on 12-well plates (1×10^6 cells per well) and cultured in serum-free medium for 24 hours with control buffer, AM, or AM plus wortmannin, a PI3K inhibitor (50 nmol/L). TUNEL for detection of apoptotic nuclei was performed according to the manufacturer's instructions. MNCs were then mounted in medium that contained 4′,6-diamidino-2-phenylindole (DAPI). Randomly selected microscopic fields (n=10) were evaluated to calculate the ratio of TUNEL-positive cells to total cells.

Adhesion Assay

We evaluated whether AM enhances MNC adhesiveness according to a previously reported method.[13] In brief, human umbilical vein endothelial cells (HUVECs) were cultured to confluence on 6-well plates with or without pretreatment with tumor necrosis factor-α (1 ng/mL). In the absence or presence of AM (10^{-7} mol/L), 1×10^6 MNCs labeled with PKH26 were incubated on an HUVEC monolayer for 24 hours. Nonadherent MNCs were removed, and the number of PKH26-positive cells in each well was counted.

Cell ELISA

Expression of adhesion molecules in HUVECs was measured by cell ELISA, as reported previously.[14] In brief, confluent HUVECs on 96-well plates were treated with AM (10^{-7} mol/L) or control buffer for 4 hours. HUVECs were then incubated with monoclonal mouse antibodies against intercellular adhesion molecule-1 (ICAM-1, R&D Systems) and vascular adhesion molecule-1 (VCAM-1, R&D Systems). A protein detector ELISA kit (KPL) was used to detect bound monoclonal antibodies.

EPC Culture Assay

Culture of EPCs was performed as described previously.[11,15,16] In brief, 2×10^6 MNCs were plated in Medium-199 supplemented with 20% FCS, heparin, and antibiotics on fibronectin-coated 6-well plates. AM (10^{-7} mol/L), human recombinant vascular endothelial growth factor (VEGF; 20 ng/mL), or control buffer was added to each plate. After 7 days of culture, nonadherent cells were removed, and adherent cells were incubated with acetylated LDL labeled with DiI (DiI-acLDL, Biomedical Technologies) and FITC-labeled lectin from ulex europaeus (Sigma). Double-positive cells for DiI-acLDL and FITC-labeled lectin were identified as EPCs.[16] Randomly selected microscopic fields (n=10) were evaluated to count the number of EPCs.

Fluorescence-Activated Cell Sorting Analysis

Fluorescence-activated cell sorting was performed to identify characteristics of adherent cells after 7 days of culture.[16] Cells were incubated for 30 minutes at 4°C with anti-human CD31 antibodies (clone L133.1, Becton Dickinson), anti-human KDR antibodies (clone KDR-1, Sigma), and anti-human VE-cadherin antibodies (clone BV6, Chemicon). Isotype-identical antibodies served as controls. Fluorescence-activated cell sorting analyses were performed with a FACSCalibur flow cytometer and Cell Quest software (BD Biosciences).

Real-Time Polymerase Chain Reaction

Expression of calcitonin receptor-like receptor (CRLR), a receptor for AM, was examined by real-time polymerase chain reaction (PCR). Total RNA was extracted from MNCs, EPCs, and HUVECs with an RNA extraction kit (RNeasy Mini Kit, Qiagen) and converted to cDNA by reverse transcription. Real-time PCR was performed with SYBR green dye (QuantiTect SYBR Green PCR kit, Qiagen) and a Prism 7700 sequence detection system (Applied Biosystems). The PCR primers for CRLR were as follows: sense primer 5′-CATTCAACAAGCAGAAGGCG-3′ and antisense primer 5′-AGCCATCCATCCCAGGTTC-3′. For GAPDH, the primers were as follows: sense primer 5′-CAATGCCTCCTGCACCACCAA-3′ and antisense primer 5′-GAGGCAGGGATGATGTTCTGGA-3′. Levels of CRLR mRNA were normalized to that of